Electronic Supplementary Material (ESI) for Physical Chemistry Chemical Physics.
This journal is © the Owner Societies 2023

Hydrogen-bonding and resonance stabilisation effects in cationic bis(iminium) phenoxide diacids

Supporting Information

Rebecca L. Jones[1], Louis J. Morris[1], Clement G. Collins Rice[1], Zoë R. Turner[1], John E. McGrady[2] and Dermot O'Hare[1]*

[1]*Chemistry Research Laboratory, Department of Chemistry, University of Oxford, Mansfield Road, Oxford, OX1 3TA, United Kingdom. Tel: +44(0) 1865 285157; E-mail: dermot.ohare@chem.ox.ac.uk.*

[2]*Inorganic Chemistry Laboratory, Department of Chemistry, University of Oxford, Oxford OX1 3QR, U.K,*

Email: john.mcgrady@chem.ox.ac.uk

Table of Contents

I. General considerations

Air and moisture sensitive manipulations were carried out using standard Schlenk line or drybox techniques under an atmosphere of dinitrogen. Protio solvents, for use in air and moisture sensitive manipulations, were degassed by sparging with dinitrogen, dried by passing through a column of activated sieves using an MBraun SPS-800 solvent purification system (pentane, benzene) and stored over potassium mirrors, or distilled from sodium metal and stored over activated 4 Å molecular sieves (THF) or over a potassium mirror (diethyl ether). Deuterated solvents (chloroform-*d*, THF-d_8, methanol-*d*, ethanol-*d*, acetonitrile-d_3) were dried over CaH_2, distilled under reduced pressure, and freeze-pump-thaw degassed three times prior to use.

The syntheses of 2,6-diformyl-4-*tert*-butyl phenol,[1, 2] $H^{tBu,Dipp}L$,[3] $[Na(OEt_2)_3][H_2N\{B(C_6F_5)_3\}_2]$[4] and $[H(OEt_2)_2][H_2N\{B(C_6F_5)_3\}_2]$[4] were adapted from literature procedures. 4-*tert*-butyl phenol (Fluorochem), hexamethylenetetramine (Sigma Aldrich), trifluoroacetic acid (Fluorochem), *p*-toluenesulfonic acid (Sigma Aldrich), 2,6-diisopropyl aniline (Apollo Scientific), sodium amide (Sigma Aldrich) and tris(pentafluorophenyl)borane (Alfa Aesar) were all used as received. HCl (1.0 M in diethyl ether; VWR) and tetrafluoroboric acid diethyl ether complex (stored only in plastic; Sigma Aldrich) were stored at 4 °C and used as received. Other reagents and solvents were used as received.

Solution NMR spectra were recorded at 298 K, unless otherwise stated, on Bruker AVIII 400 nanobay, Bruker AVIII 500, or Bruker NEO 600 spectrometers. Two dimensional ^{1}H-^{1}H and ^{13}C-^{1}H correlation experiments were used, when necessary, to confirm ^{1}H and ^{13}C assignments. ^{19}F and ^{11}B solution NMR spectra were also recorded on the same spectrometers at operating frequencies of 377 or 470 and 128 or 160 MHz respectively. ^{1}H and ^{13}C NMR spectra were referenced internally to residual protio solvent and are reported relative to tetramethylsilane (δ

= 0 ppm). ^{19}F and ^{11}B were referenced externally to $CFCl_3$ in $CDCl_3$ and $BF_3(OEt_2)$ respectively. Chemical shifts are quoted in δ (ppm) and coupling constants in Hertz. Air sensitive samples were prepared in a glovebox under an inert atmosphere, using dried deuterated solvents in J. Young's NMR tubes.

Fourier transform infrared (FTIR) spectroscopy samples were prepared in a glove box as pellets using anhydrous potassium bromide (KBr). IR spectra were recorded on a Nicolet iS5 ThermoScientific spectrometer (range = 4000–400 cm^{-1} with resolution = 1 cm^{-1}) in transmission mode. A background spectrum was run prior to the sample and was subtracted from the sample spectra.

Elemental analyses (CHN) were carried out in duplicate at London Metropolitan University by Miss Orla McCullough.

II. Additional synthetic and characterisation details

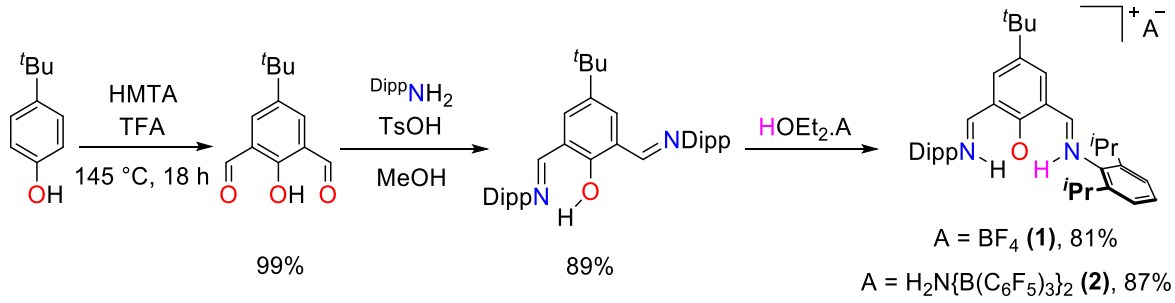

Scheme S1. Overview of the synthesis of $[H_2{}^{tBu,Dipp}L][A]$ **(1-2)**.

Synthesis of 2,6-diformyl-4-*tert*-butyl phenol; adapted from[1, 2]

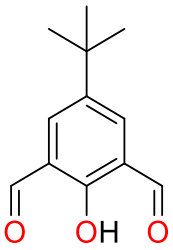

A mixture of 4-*tert*-butyl phenol (5.00 g, 1.0 eq.) and hexamethylenetetramine (2.0 eq) in trifluoroacetic acid (15.0 eq.) was heated at 145 ºC for 18 h. The resultant hot dark brown solution was poured into 4 N HCl (115 mL) and stirred at room temperature for 2 h. The reaction mixture was then stored overnight at 5 °C before the precipitate was isolated via filtration. The crude product was washed with ice-cold distilled water (3 x 50 mL) and -78 °C methanol (3 x 20 mL) affording the desired aldehyde as a bright yellow solid. A second crop of pure material crystallised overnight from the room temperature washings (combined mass: 6.77 g, combined yield: 99%). ^{1}H NMR (400 MHz, 298 K, chloroform-*d*): δ 11.47 (s, 1H, O***H***), 10.24 (s, 2H, ***H***CO), 7.98 (s, 2H, 3,5-C$_6$***H***$_3$), 1.35 (s, 9H, C(C***H***$_3$)$_3$) ppm; these spectroscopic values are consistent with previous literature reports.[1]

Synthesis of H$^{t\text{Bu,Dipp}}$L; adapted from[3]

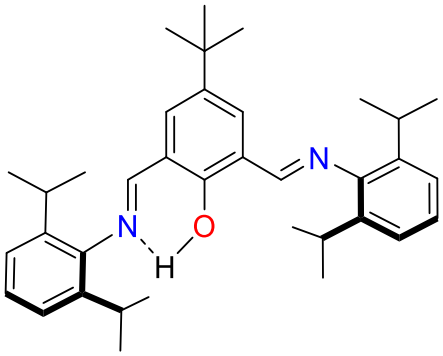

A solution of 2,6-diformyl-4-*tert*-butyl phenol (0.500 g, 1.0 eq.) and 2,6-diisopropylaniline (2.0 eq.) in methanol (10 mL) was prepared. *p*-Toluenesulfonic acid (0.0500 g, 0.263 mmol) was added to the solution and the resultant mixture was stirred at room temperature overnight. The precipitate that had formed during this time was isolated via filtration and washed with ice-cold methanol (2 x 5 mL) to yield the desired bis(imino)phenol as a pale-yellow powder (1.13 g, 89%). ^{1}H NMR (500 MHz, 223 K, chloroform-*d*): δ 13.64 (s, 1H, O***H***), 8.80 (s, 1H, ***H***C=N'), 8.42 (d, $^4J_{HH}$ = 2.5 Hz, 1H, 3'-C$_6$***H***$_2$), 8.39 (s, 1H, ***H***C=N), 7.53 (d, $^4J_{HH}$ = 2.6 Hz, 1H, 3-C$_6$***H***$_2$), 7.25-7.14 (overlapping m, 6H, N$^{(')}$-3,4,5-C$_6$***H***$_3$), 2.99 (overlapping sept, $^3J_{HH}$ = 6.8, 7.0 Hz, 4H, N$^{(')}$-2,6-C$_6$H$_3$-C***H***Me$_2$), 1.42 (s, 9H, C(C***H***$_3$)$_3$), 1.19

(dd, $^{3}J_{HH}$ = 6.9, 6.9 Hz, 24H, N$^{(')}$-2,6-C_6H_3-CH***Me***$_2$) ppm. $^{13}C\{^{1}H\}$ NMR (125 MHz, 223 K, chloroform-*d*): δ 166.5 (H***C***=N), 159.5 (1-***C***$_6H_2$), 157.6 (H***C***=N'), 149.4 (N'-1-***C***$_6H_3$), 145.5 (N-1-***C***$_6H_3$), 141.7 (4-***C***$_6H_2$), 138.5-137.8 (N-3,5-***C***$_6H_3$ and N'-3,5-***C***$_6H_3$), 132.5 (3-***C***$_6H_2$), 127.5 (3'-***C***$_6H_2$), 125.5 (N-4-***C***$_6H_3$ and N'-4-***C***$_6H_3$), 124.0 (2'-***C***$_6H_2$), 123.2-123.0 (N-2-***C***$_6H_3$ and N'-2-***C***$_6H_3$), 118.5 (2-***C***$_6H_2$), 34.4 (***C***$(CH_3)_3$), 31.4 (C(***C***$H_3)_3$), 28.0-27.8 (N-2,6-C_6H_3-***C***HMe_2 and N'-2,6-C_6H_3-***C***HMe_2), 23.8 (N-2,6-C_6H_3-CH***Me***$_2$ and N'-2,6-C_6H_3-CH***Me***$_2$) ppm. IR (KBr): 3064, 3018, 2962, 2924, 2868, 1628, 1585, 1459, 1362, 1311, 1178, 1108, 1031, 1007, 932, 869, 856, 786, 756 cm^{-1}. Anal. Calcd for $C_{36}H_{48}N_2O$: C, 82.39; H, 9.22; N, 5.34. Found: C, 83.92; H, 9.31; N, 5.33. These spectroscopic values are consistent with previous literature reports.[3]

Synthesis of [$H_2{}^{t\text{Bu,Dipp}}$L][BF_4].thf$_x$ (1)

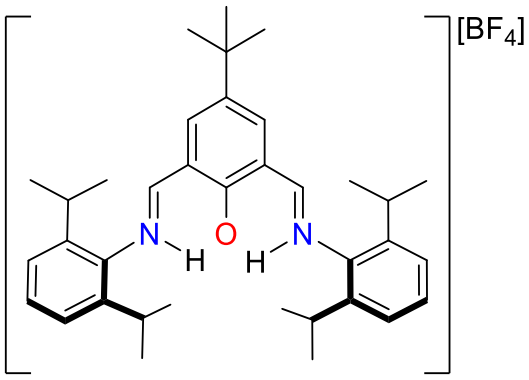

[$H(OEt)_2$][BF_4] (130 µL, 0.953 mmol) was added to a solution of H$^{t\text{Bu,Dipp}}$L (0.500 g, 0.953 mmol) in THF (5 mL). The bright orange reaction mixture was then left stirring for 3 h at room temperature before volatiles were removed *in vacuo*. The crude oily solid was washed by sonication in pentane (3 x 15 mL) and filtered to afford the desired product as a bright orange solid. The bulk material had the composition [$H_2{}^{t\text{Bu,Dipp}}$L][BF_4]·thf$_4$ (0.694 g, 81%). ^{1}H NMR (500 MHz, 298 K, THF-d_8): δ 15.05 (d, $^{3}J_{HH}$ = 13.5 Hz, 2H, N***H***), 9.04 (d, $^{3}J_{HH}$ = 13.3 Hz, 2H, ***H***C=N), 8.42 (s, 2H, 3-C_6***H***$_2$), 7.44 (dd, $^{3}J_{HH}$ = 8.5, 7.0 Hz, 2H, N-4-C_6***H***$_3$), 7.35 (d, $^{3}J_{HH}$ = 7.8 Hz, 4H, N-3,5-C_6***H***$_3$), 3.37 (m, 16H, thf-OC***H***$_2$), 3.14 (sept, $^{3}J_{HH}$ = 6.7 Hz, 4H, N-2,6-C_6H_3-C***H***Me_2), 1.59 (m, 16H, thf-C***H***$_2$), 1.36 (s, 9H, C(C***H***$_3)_3$), 1.25 (d, $^{3}J_{HH}$ = 6.8 Hz, 24H, N-2,6-C_6H_3-CH***Me***$_2$) ppm. $^{13}C\{^{1}H\}$ NMR (151 MHz, 298 K, THF-d_8): δ 178.1 (1-***C***$_6H_2$), 171.0 (H***C***=N), 145.5 (3-***C***$_6H_2$), 143.3 (N-

2,6-***C***$_6$H$_3$), 139.3 (4-***C***$_6$H$_2$), 134.4 (N-1-***C***$_6$H$_3$), 129.8 (N-4-***C***$_6$H$_3$), 124.0 (N-3,5-***C***$_6$H$_3$), 117.4 (2-***C***$_6$H$_2$), 69.3 (thf-O***C***H$_2$), 34.0 (***C***(CH$_3$)$_3$), 30.3 (C(***C***H$_3$)$_3$), 28.6 (N-2,6-C$_6$H$_3$-***C***HMe$_2$), 25.5 (thf-***C***H$_2$), 22.8 (N-2,6-C$_6$H$_3$-CH***Me***$_2$) ppm. ^{19}F NMR (377 MHz, 298 K, THF-d_8): δ -150.69 ppm. ^{11}B NMR (128 MHz, 298 K, THF-d_8): δ -0.96 ppm. IR (KBr): 3061, 3045, 2966, 2931, 2869, 2856, 1659, 1623, 1586, 1530, 1464, 1389, 1368, 1329, 1292, 1237, 1186, 1108, 1058, 1020, 937, 901, 801, 768, 756 cm^{-1}. Anal. Calcd for $C_{36}H_{49}N_2OBF_4$: C, 70.58; H, 8.06; N, 4.57. Found: C, 70.91; H, 8.52; N, 4.31. Single crystals of [H$_2$$^{t\text{Bu,Dipp}}$L][BF$_4$], suitable for an X-ray diffraction study, were obtained by the slow evaporation of a saturated benzene solution at room temperature.

Synthesis of [Na(OEt$_2$)$_3$][H$_2$N{B(C$_6$F$_5$)$_3$}$_2$]; adapted from[4]

At 0 °C, a slurry of B(C$_6$F$_5$)$_3$ (2.10 g, 4.10 mmol) in diethyl ether (25 mL) was added to a slurry of NaNH$_2$ (0.0800 g, 2.05 mmol) in diethyl ether (5 mL). The reaction mixture was then warmed to room temperature and stirred for 2 h. The solution was concentrated until crystallisation was initiated and the resultant glassy solid was washed with -78 °C diethyl ether (3 x 5 mL) to afford the desired product as a colourless powder (1.32 g, 50%). ^{1}H NMR (400 MHz, 298 K, chloroform-*d*) δ 5.64 (s (br), 2H, [***H***$_2$N{B(C$_6$F$_5$)$_3$}$_2$]$^-$), 3.57 (q, $^3J_{HH}$ = 7.1 Hz, 12H, OC***H***$_2$CH$_3$), 1.20 (t, $^3J_{HH}$ = 7.1 Hz, 18H, OCH$_2$C***H***$_3$) ppm. ^{19}F NMR (377 MHz, 298 K, chloroform-*d*) δ -132.8 (d, $^3J_{FF}$ = 20.7 Hz, 12F, *o*-F:C$_6$***F***$_5$), -159.1 (t, $^3J_{FF}$ = 20.6 Hz, 6F, *p*-F:C$_6$***F***$_5$), -165.2 (t, $^3J_{FF}$ = 21.2 Hz, 12F, *m*-F:C$_6$***F***$_5$) ppm. ^{11}B NMR (128 MHz, 298 K, chloroform-*d*) δ -8.3 ppm; all of these spectroscopic values are consistent with previous literature reports.[4]

Synthesis of [H(OEt$_2$)$_2$][H$_2$N{B(C$_6$F$_5$)$_3$}$_2$]; adapted from[4]

A solution of [Na(OEt$_2$)$_3$][H$_2$N{B(C$_6$F$_5$)$_3$}$_2$] (2.20 g, 1.71 mmol) in diethyl ether (10 mL) was prepared. To this was added an excess of HCl (1.0 M in diethyl ether, 3.42 mL, 2.0 eq). The

reaction mixture was stirred at room temperature for 18 h prior to filtration. Removal of volatiles *in vacuo* afforded a crude oily solid which, when washed under rapid stirring with pentane (15 mL), yielded the desired product as a colourless solid (1.84 g, 90%). ^{1}H NMR (400 MHz, 298 K, chloroform-*d*) δ 5.65 (s (br), 2H, [***H***$_2$N{B(C$_6$F$_5$)$_3$}$_2$]$^-$), 4.10 (q, $^3J_{HH}$ = 7.3 Hz, 8H, OC***H***$_2$CH$_3$), 1.46 (t, $^3J_{HH}$ = 7.2 Hz, 12H, OCH$_2$C***H***$_3$) ppm. ^{19}F NMR (377 MHz, 298 K, chloroform-*d*) δ -132.5 (d, $^3J_{FF}$ = 20.8 Hz, 12F, *o*-F:C$_6$***F***$_5$), -159.5 (t, $^3J_{FF}$ = 20.4 Hz, 6F, *p*-F:C$_6$***F***$_5$), -165.1 (t, $^3J_{FF}$ = 21.3 Hz, 12F, *m*-F:C$_6$***F***$_5$) ppm. ^{11}B NMR (128 MHz, 298 K, chloroform-*d*) δ -8.3 ppm; all of these spectroscopic values are consistent with previous literature reports.[4]

Synthesis of [H$_2$$^{t\text{Bu,Dipp}}$L][H$_2$N{B(C$_6F_5$)$_3$}$_2$] (2)

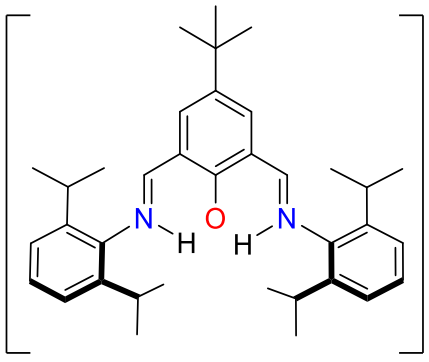

[H$_2$N{B(C$_6$F$_5$)$_3$}$_2$]

A solution of [H(OEt$_2$)$_2$][H$_2$N{B(C$_6$F$_5$)$_3$}$_2$] (0.456 g, 0.381 mmol) in THF (3 mL) was added dropwise to a solution of H$^{t\text{Bu,Dipp}}$L (0.200 g, 0.381 mmol) in THF (2 mL). The bright orange reaction mixture was then left to stir for 3 h at room temperature before volatiles were removed *in vacuo*. The crude oily solid was triturated with a 1:1 mixture of pentane:diethyl ether (4 x 5 mL) to afford the desired product as a bright orange solid. The bulk material had the composition [H$_2$$^{t\text{Bu,Dipp}}$L][H$_2$N{B(C$_6F_5$)$_3$}$_2$].thf$_{0.36}$ (0.528 g, 87%). ^{1}H NMR (600 MHz, THF-*d*$_8$) δ 14.90 (s (br), 2H, HC=N***H***), 8.86 (s (br), 2H, ***H***C=NH), 8.14 (s, 2H, 3-C$_6$***H***$_2$), 7.51 (t, $^3J_{HH}$ = 7.8 Hz, 2H, N-4-C$_6$***H***$_3$), 7.42 (d, $^3J_{HH}$ = 7.8 Hz, 4H, N-3,5-C$_6$***H***$_3$), 5.77 (s (br), 2H, [***H***$_2$N{B(C$_6$F$_5$)$_3$}$_2$]$^-$), 3.37 (m, 1H, thf-OC***H***$_2$), 3.11 (sept, $^3J_{HH}$ = 6.6 Hz, 4H, N-2,6-C$_6$H$_3$-C***H***Me$_2$), 1.60 (m, 1H, thf-C***H***$_2$), 1.39 (s, 9H, C(C***H***$_3$)$_3$), 1.28 (d, $^3J_{HH}$ = 6.8 Hz, 24H, N-2,6-C$_6$H$_3$-CH***Me***$_2$) ppm. ^{13}C{^{1}H} NMR (151 MHz, 298 K, THF-*d*$_8$) δ 179.2 (1-***C***$_6$H$_2$), 171.2 (H***C***=N), 149.9-148.2 (*o*-F:***C***$_6$F$_5$), 145.7 (3-***C***$_6$H$_2$), 144.4 (N-2,6-***C***$_6$H$_3$),

141.1-139.8 (*p*-F:***C***$_6$F$_5$), 139.8 (4-***C***$_6$H$_2$), 138.6-136.9 (*m*-F:***C***$_6$F$_5$), 135.7 (N-1-***C***$_6$H$_3$), 131.5 (N-4-***C***$_6$H$_3$), 125.5 (N-3,5-***C***$_6$H$_3$), 118.9 (2-***C***$_6$H$_2$), 69.3 (thf-O***C***H$_2$), 34.9 (***C***(CH$_3$)$_3$), 31.2 (C(***C***H$_3$)$_3$), 29.9 (N-2,6-C$_6$H$_3$-***C***HMe$_2$), 25.5 (thf-***C***H$_2$), 23.8 (N-2,6-C$_6$H$_3$-CH***Me***$_2$) ppm. ^{19}F NMR (377 MHz, 298 K, THF-d_8) δ -133.1 (d, $^3J_{FF}$ = 20.8 Hz, 12F, *o*-F:C$_6$***F***$_5$), -161.0 (t, $^3J_{FF}$ = 20.2 Hz, 6F, *p*-F:C$_6$***F***$_5$), -166.3 (t, $^3J_{FF}$ = 20.0 Hz, 12F, *m*-F:C$_6$***F***$_5$) ppm. ^{11}B NMR (128 MHz, 298 K, THF-d_8) δ -8.2 ppm. IR (KBr): 3383, 3344, 3073, 2974, 2933, 2875, 2362, 2334, 1647, 1622, 1519, 1461, 1369, 1329, 1275, 1228, 1103, 1085, 986, 953, 885, 800, 779, 764, 715, 692, 652, 619, 517756 cm^{-1}. Anal. Calcd for C$_{74.27}$H$_{54.15}$N$_3$O$_{1.41}$B$_2$F$_{30}$ (sample contained residual protio-solvent: 0.4 eq THF and 0.1 eq pentane): C, 55.66; H, 3.41; N, 2.62. Found: C, 55.81; H, 3.59; N, 2.63. Single crystals of [H$_2$$^{t\text{Bu,Dipp}}$L][H$_2$N{B(C$_6F_5$)$_3$}$_2$], suitable for an X-ray diffraction study, were obtained from a dichloromethane/pentane mixture at -25 ºC.

Synthesis of [pyrazole-H][H$_2$N{B(C$_6$F$_5$)$_3$}$_2$] (3)

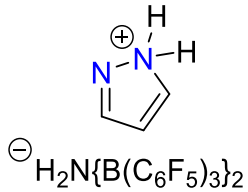

A solution of [H(OEt$_2$)$_2$][H$_2$N{B(C$_6$F$_5$)$_3$}$_2$] (0.176 g, 0.147 mmol) in THF (3 mL) was added dropwise to a solution of pyrazole (0.010 g, 0.147 mmol) in THF (2 mL). The pale-yellow reaction mixture was then left to stir for 1 h at room temperature before volatiles were removed *in vacuo*. The crude oily solid was washed with cold pentane (3 x 5 mL) to afford the desired product as an off-white powder. The bulk material had the composition [pyrazole-H(OEt$_2$)$_{0.75}$][H$_2$N{B(C$_6$F$_5$)$_3$}$_2$] (0.139 g, 81%). ^{1}H NMR (400 MHz, acetonitrile-d_3) δ 12.52 (s, 2H, N***H***$_2$), 8.09 (d, $^3J_{HH}$ = 2.8 Hz, 2H, C1,C3-***H***), 6.76 (t, $^3J_{HH}$ = 2.7 Hz, 1H, C2-***H***), 5.77 (s (br), 2H, [***H***$_2$N{B(C$_6$F$_5$)$_3$}$_2$]$^-$) ppm. ^{13}C{^{1}H} NMR (151 MHz, 298 K, acetonitrile-d_3) δ 149.6 (***C***1,***C***3), 148.0 (***C***2), 141.0-139.3 (*o*-F:***C***$_6$F$_5$), 138.5-136.8 (*p*-F:***C***$_6$F$_5$), 135.7 (*m*-F:***C***$_6$F$_5$), 66.3 (diethyl ether-***C***H$_2$), 15.6 (diethyl ether-***C***H$_3$). ppm. ^{19}F NMR (377 MHz, 298 K, acetonitrile-d_3) δ -133.7 (d, $^3J_{FF}$ = 20.3 Hz, 12F, *o*-F:C$_6$***F***$_5$), -160.6 (t, $^3J_{FF}$ = 19.7 Hz, 6F, *p*-F:C$_6$***F***$_5$), -166.6 (t, $^3J_{FF}$ = 19.4 Hz, 12F, *m*-F:C$_6$***F***$_5$) ppm. ^{11}B NMR (128 MHz, 298 K, acetonitrile-d_3) δ -8.3 ppm.

IR (KBr): 3431, 3384, 3347, 3176, 3161, 2990, 1648 1520, 1466, 1304, 1276, 1098, 1095, 955, 800, 780, 764, 715, 693 cm^{-1}. Anal. Calcd for $C_{42}H_{14.5}N_3B_2O_{0.75}F_{30}$: C, 43.31; H, 1.25; N, 3.61. Found: C, 43.70; H, 1.20; N, 3.60.

General procedure for NMR titrations and pK_a determinations

These experiments were performed in triplicate using the method reported by Koppel and co-workers.[5] Pyrazole (pK_a = 3.6 in THF and 9.1 in acetonitrile) was identified as a suitable basic indicator as it only initiated partial deprotonation of the diacids.[6]

1:1 mixtures of diacid and base were prepared and analysed by ^{1}H NMR spectroscopy. When separate signals were observed for conjugate acid and base, the relative integrals of the resonances were used to determine the concentration of these species in the mixture. When time-averaged signals were observed for the conjugate acid/base or conjugate base/acid couples, the chemical shifts of the individual components were then used to determine relative concentrations:

$$\frac{[base]}{[conjugate\ acid]} = \frac{|\delta_{mix} - \delta_{base}|}{|\delta_{conjugate\ acid} - \delta_{mix}|} \ \boldsymbol{OR}\ \frac{[conjugate\ base]}{[acid]} = \frac{|\delta_{mix} - \delta_{acid}|}{|\delta_{conjugate\ base} - \delta_{mix}|}$$

The ΔpK_a values, relative to the base used, were then computed using the following equation:

$$\Delta pK_a = \log\left(\frac{[acid][base]}{[conjugate\ acid][conjugate\ base]}\right)$$

Poor solubility of **1** in acetonitrile, the typical solvent for non-aqueous acid-base chemistry, led to its acid dissociation constant being determined instead in THF.[7] On the NMR time-scale, well-defined and identifiable resonances for both pyrazole and its protonated form were observable (e.g. 6.3 and 6.6 ppm respectively); on the other hand, fast exchange between **1** and its conjugate base resulted in the detection of a time-averaged signal (see **Figure S25**). In contrast to **1**, the diacid **2**, was fully soluble in acetonitrile. In this titration, time-averaged signals were observed for both couples (see **Figure S26**).

III. Representative NMR and IR spectra

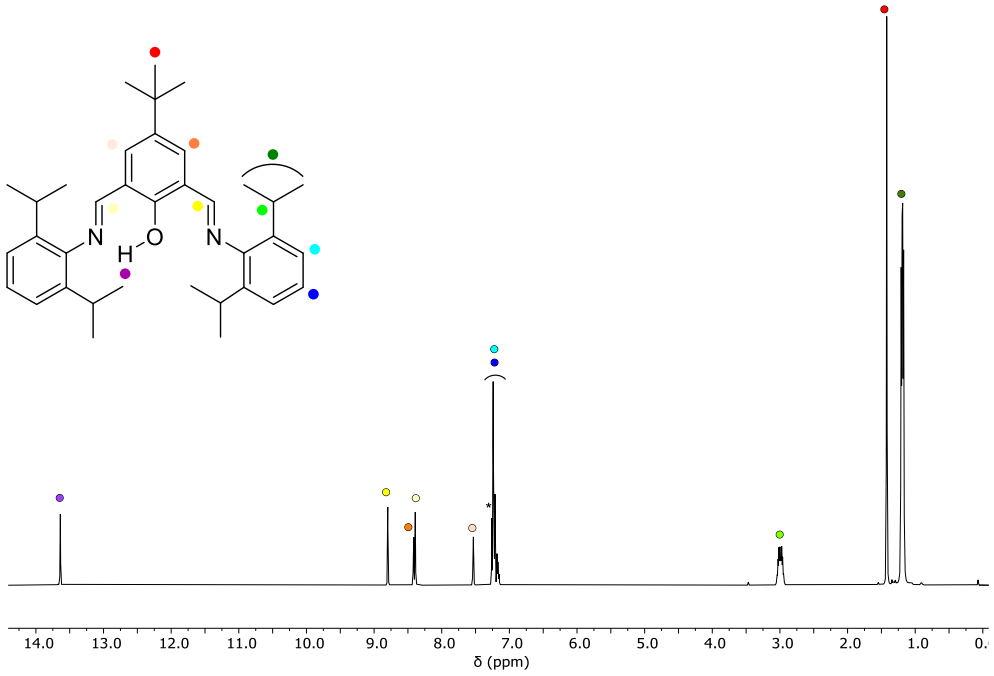

Figure S1. ^{1}H NMR spectrum (chloroform-*d*, 500 MHz, 223 K) of H$^{t\text{Bu,Dipp}}$L. * denotes residual protio solvent fraction of chloroform-*d*.

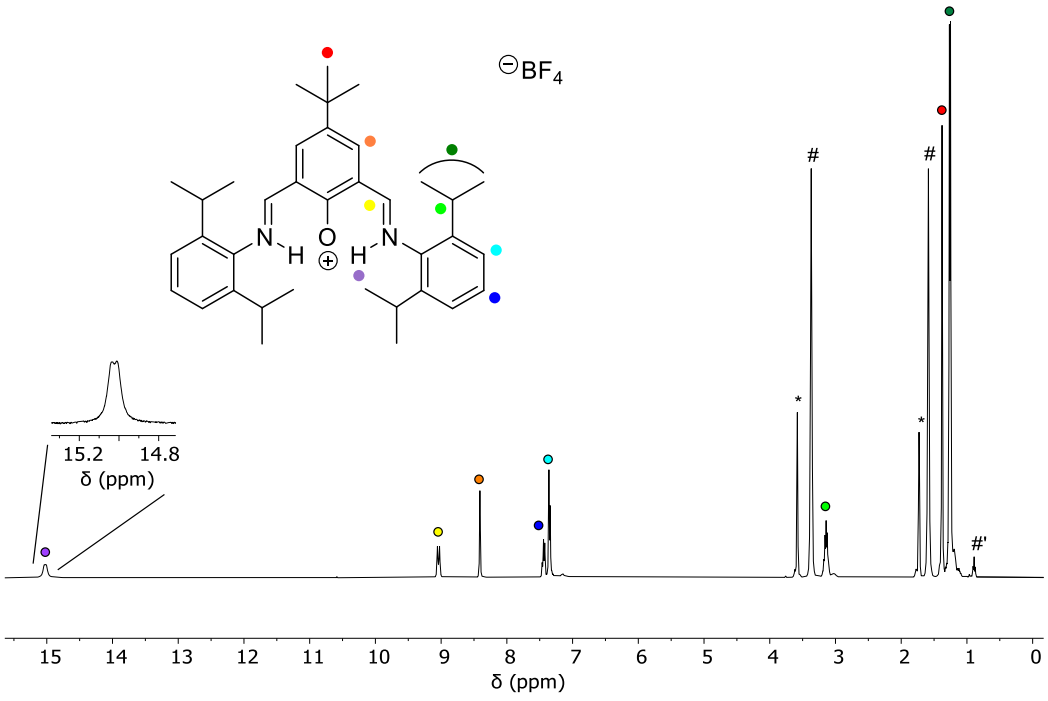

Figure S2. ^{1}H NMR spectrum (THF-d_8, 400 MHz, 298 K) of [H$_2$$^{t\text{Bu,Dipp}}$L][BF$_4$]. * denotes residual protio solvent fraction of THF-d_8. # and #' denote residual protio THF and pentane from reaction work-up.

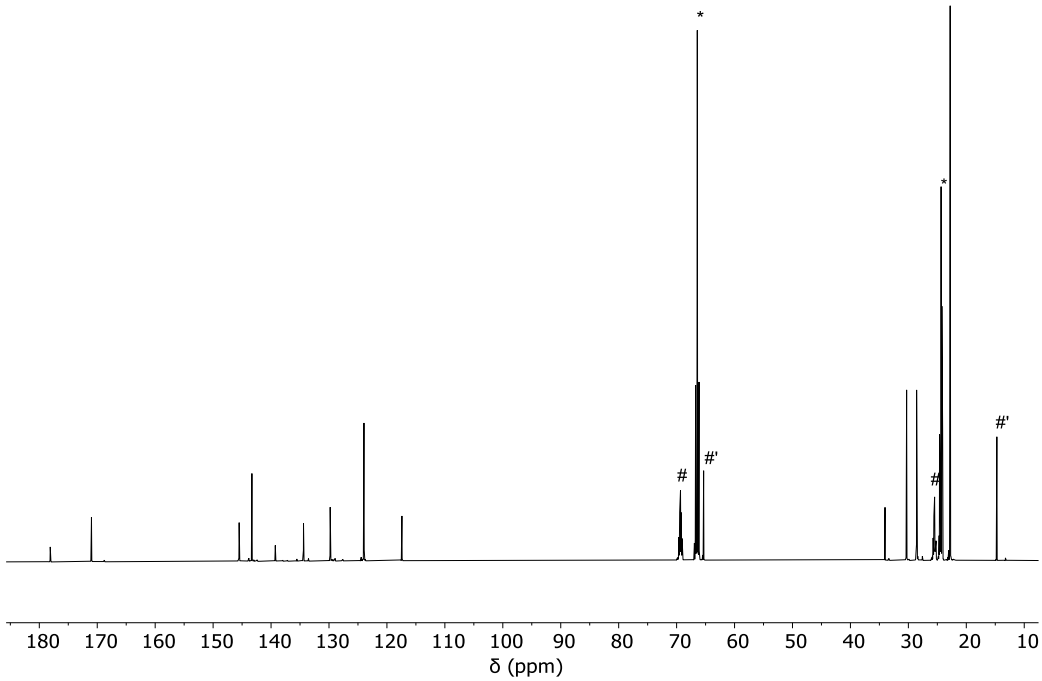

Figure S3. $^{13}C\{^{1}H\}$ NMR spectrum (THF-d_8, 151 MHz, 298 K) of $[H_2{}^{t\text{Bu,Dipp}}L][BF_4]$. * denotes residual protio solvent fraction of thf-d_8. # and #' denote residual protio THF and diethyl ether.

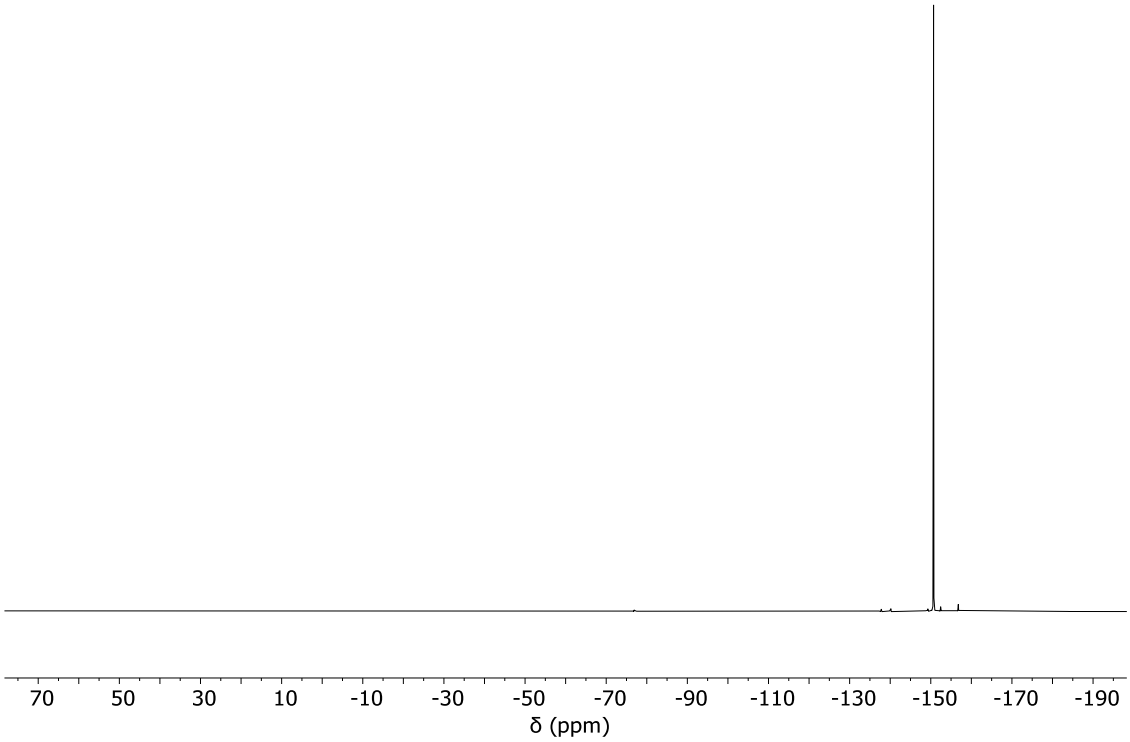

Figure S4. ^{19}F NMR spectrum (THF-d_8, 377 MHz, 298 K) of $[H_2{}^{t\text{Bu,Dipp}}L][BF_4]$.

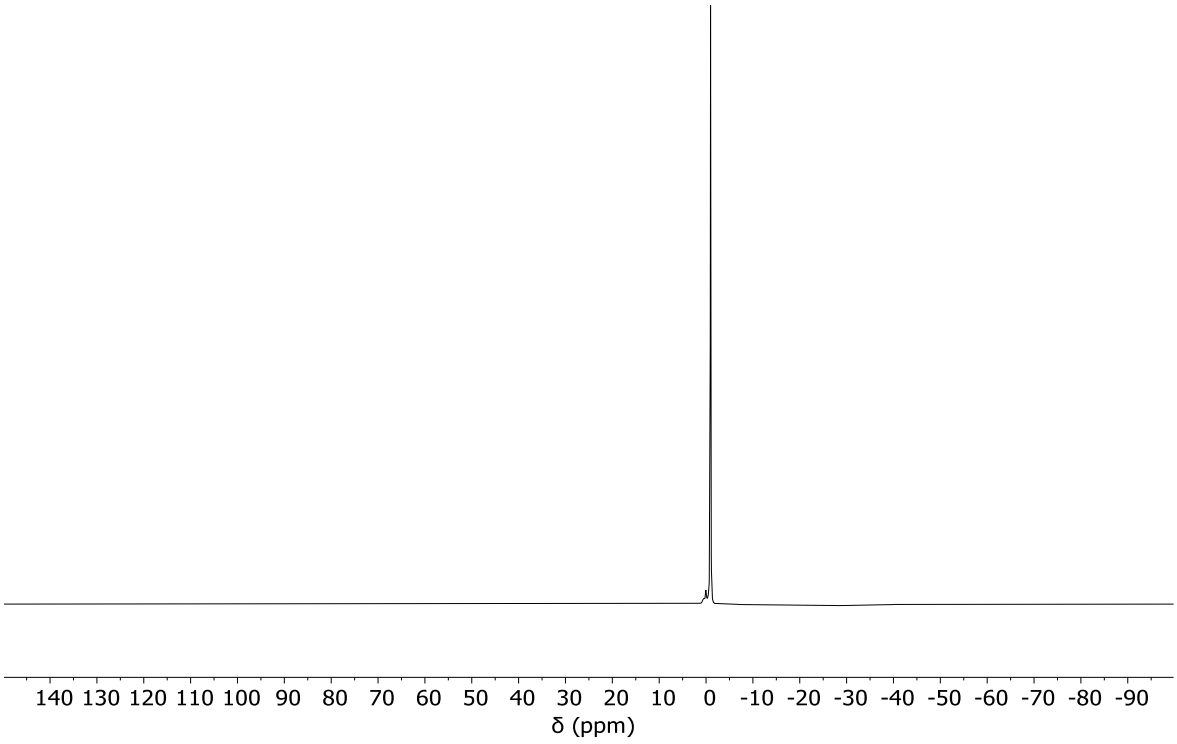

Figure S5. ^{11}B NMR spectrum (THF-d_8, 128 MHz, 298 K) of [$H_2{}^{t}$Bu,DippL][BF_4].

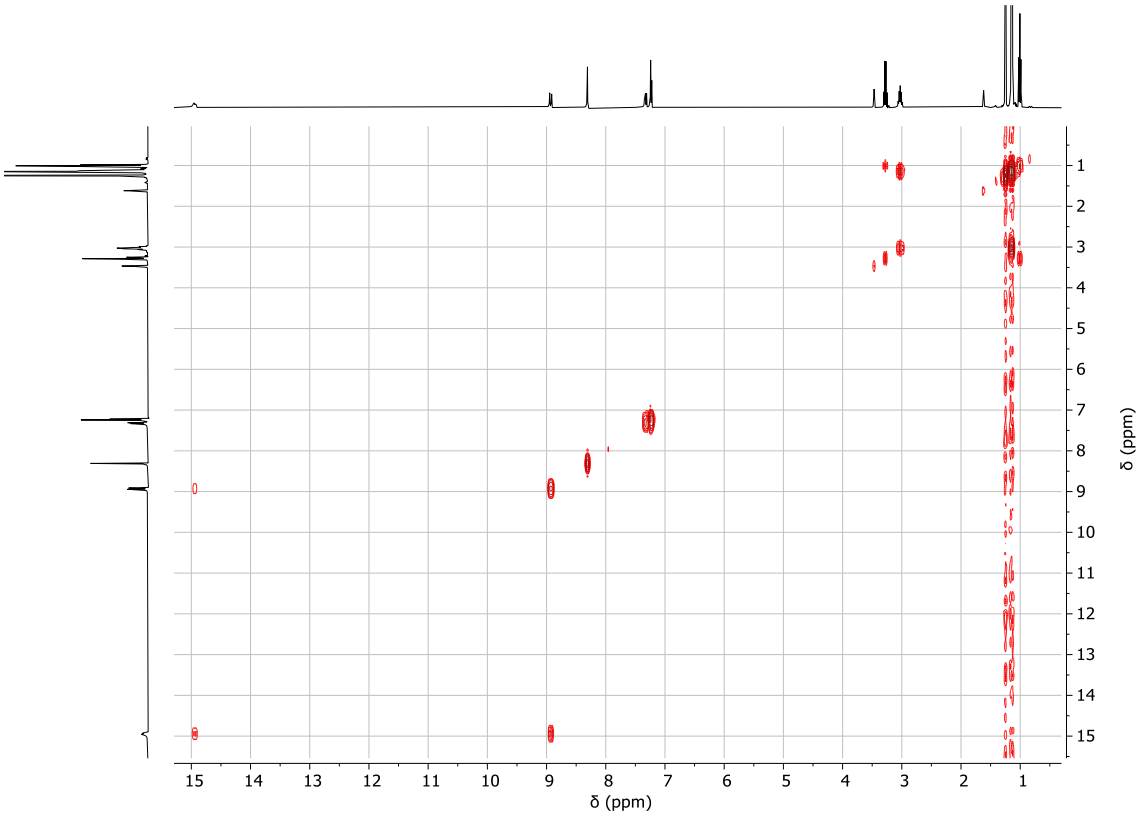

Figure S6. ^{1}H-^{1}H COSY NMR spectrum (400 MHz, THF-d_8, 298K) of [$H_2{}^{t}$Bu,DippL][BF_4].

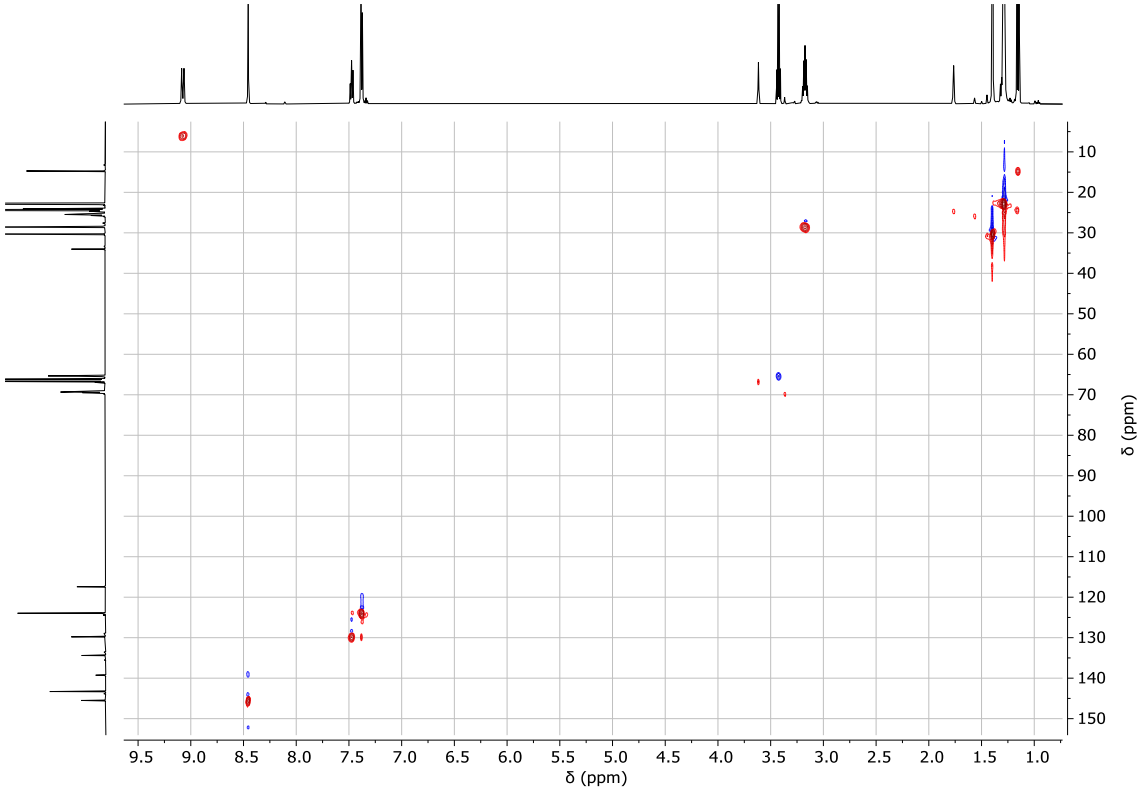

Figure S7. ^{1}H-^{13}C HSQC NMR spectrum (600 MHz, THF-d_8, 298K) of $[H_2{}^{t\text{Bu,Dipp}}L][BF_4]$.

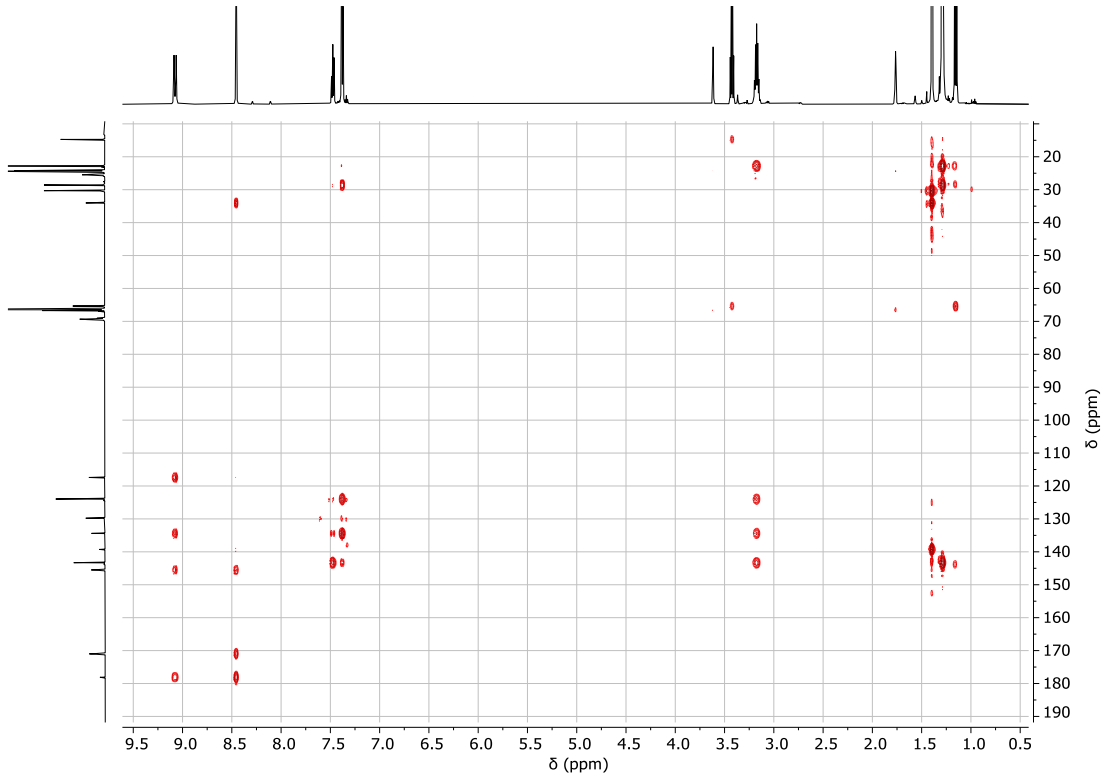

Figure S8. ^{1}H-^{13}C HMBC NMR spectrum (600 MHz, THF-d_8, 298K) of $[H_2{}^{t\text{Bu,Dipp}}L][BF_4]$.

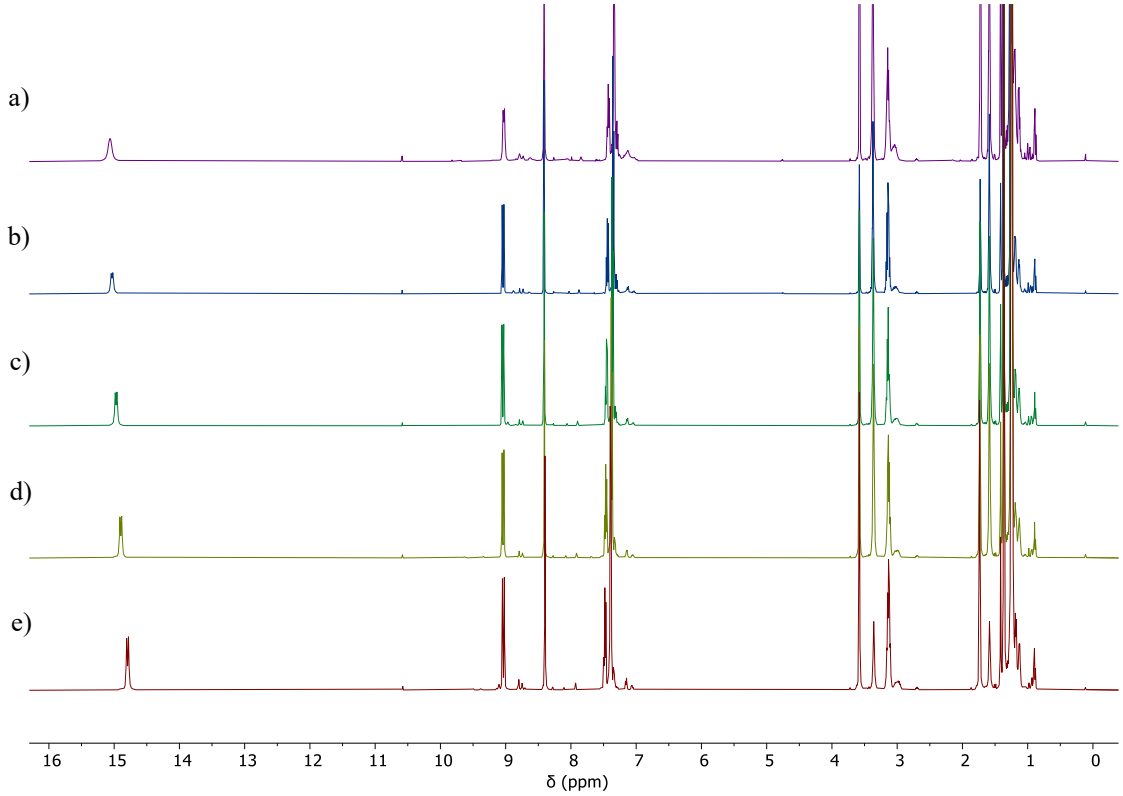

Figure S9. ^{1}H NMR spectra (500 MHz, THF-d_8) of [$H_2{}^{t\text{Bu,Dipp}}$L][BF_4] at a) 323 K, b) 298 K, c) 273 K, d) 253 K and e) 233 K.

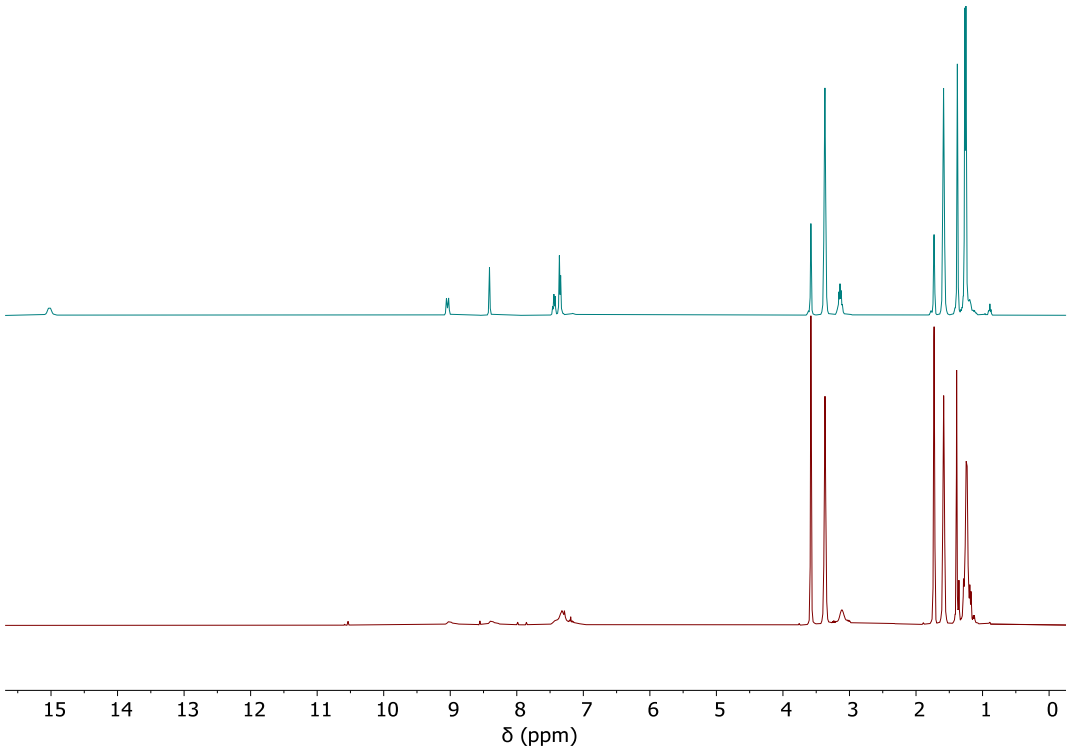

Figure S10. Comparison ^{1}H NMR spectra (400 MHz, THF-d_8) of [$H_2{}^{t\text{Bu,Dipp}}$L][BF_4] under N_2 (blue) and [$H_2{}^{t\text{Bu,Dipp}}$L][BF_4] after 18 h exposed to air (red).

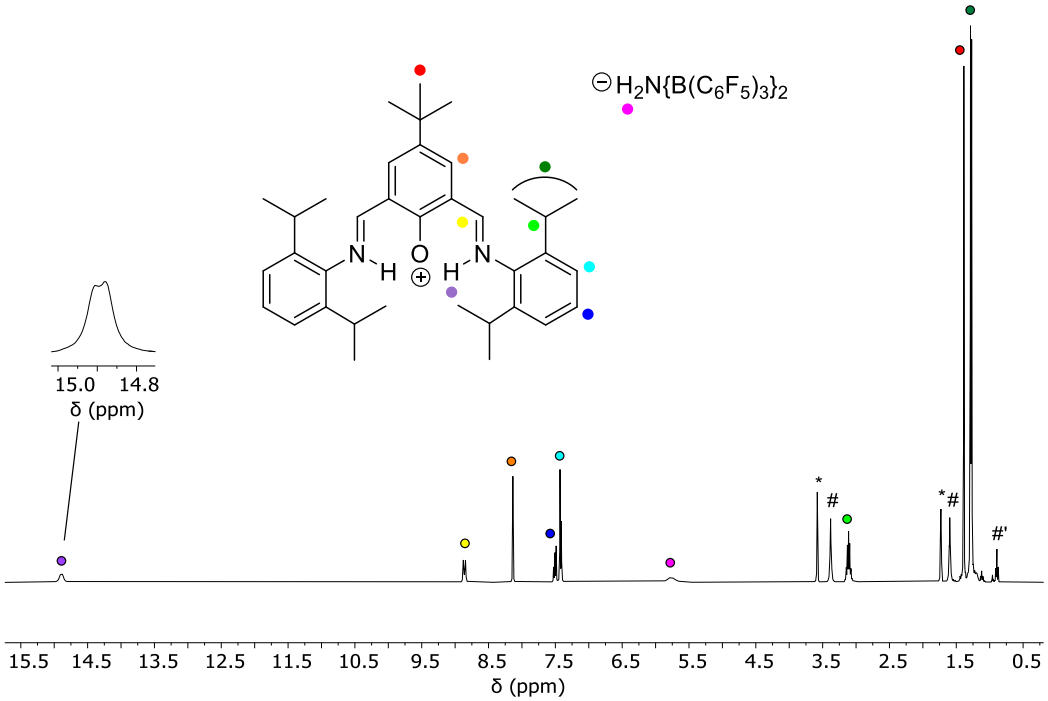

Figure S11. ^{1}H NMR spectrum (THF-d_8, 400 MHz, 298 K) of $[H_2{}^{t\text{Bu,Dipp}}L][H_2N\{B(C_6F_5)_3\}_2]$. * denotes residual protio solvent fraction of THF-d_8, # and #' denote residual protio THF and pentane from reaction work-up.

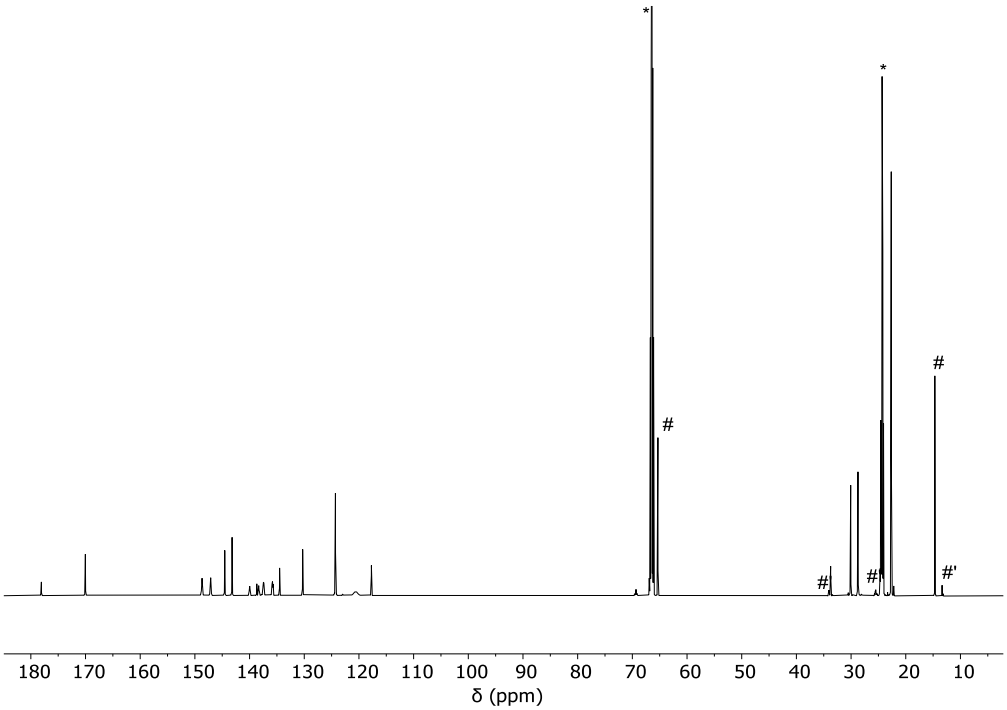

Figure S12. ^{13}C{^{1}H} NMR spectrum (THF-d_8, 151 MHz, 298 K) of $[H_2{}^{t\text{Bu,Dipp}}L][H_2N\{B(C_6F_5)_3\}_2]$. * denotes residual protio solvent fraction of THF-d_8. # and #' denote residual protio diethyl ether and pentane from reaction work-up.

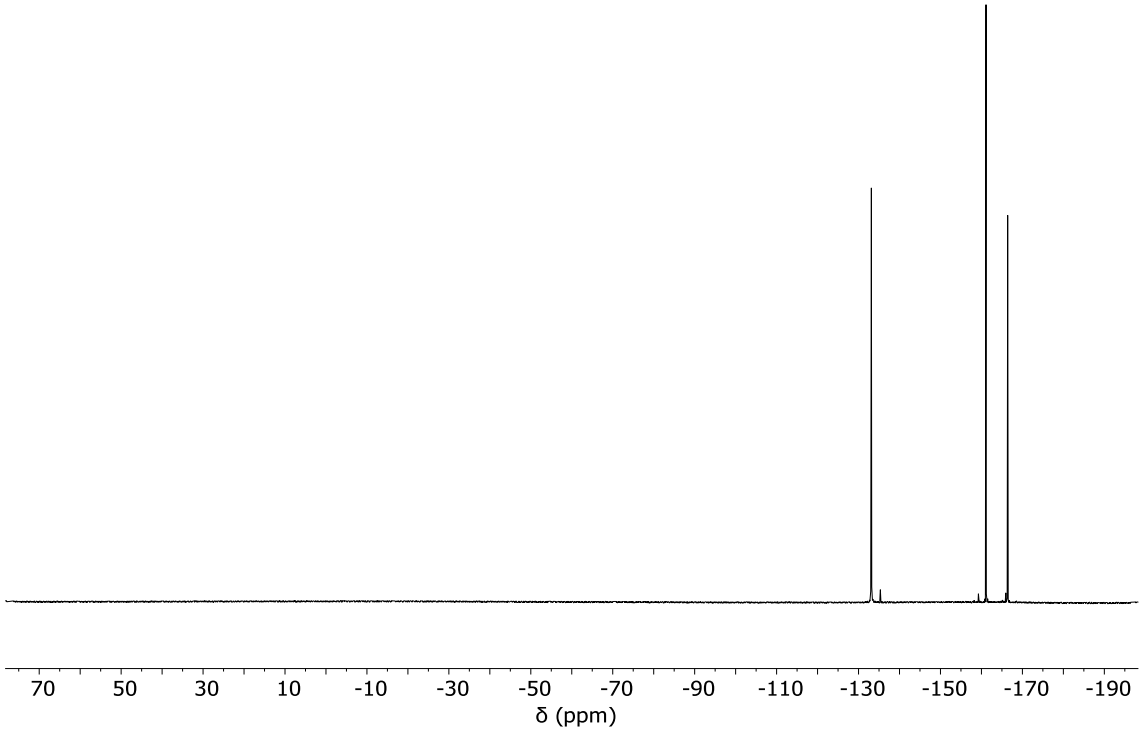

Figure S13. ^{19}F NMR spectrum (THF-d_8, 377 MHz, 298 K) of $[H_2{}^{t\text{Bu,Dipp}}L][H_2N\{B(C_6F_5)_3\}_2]$.

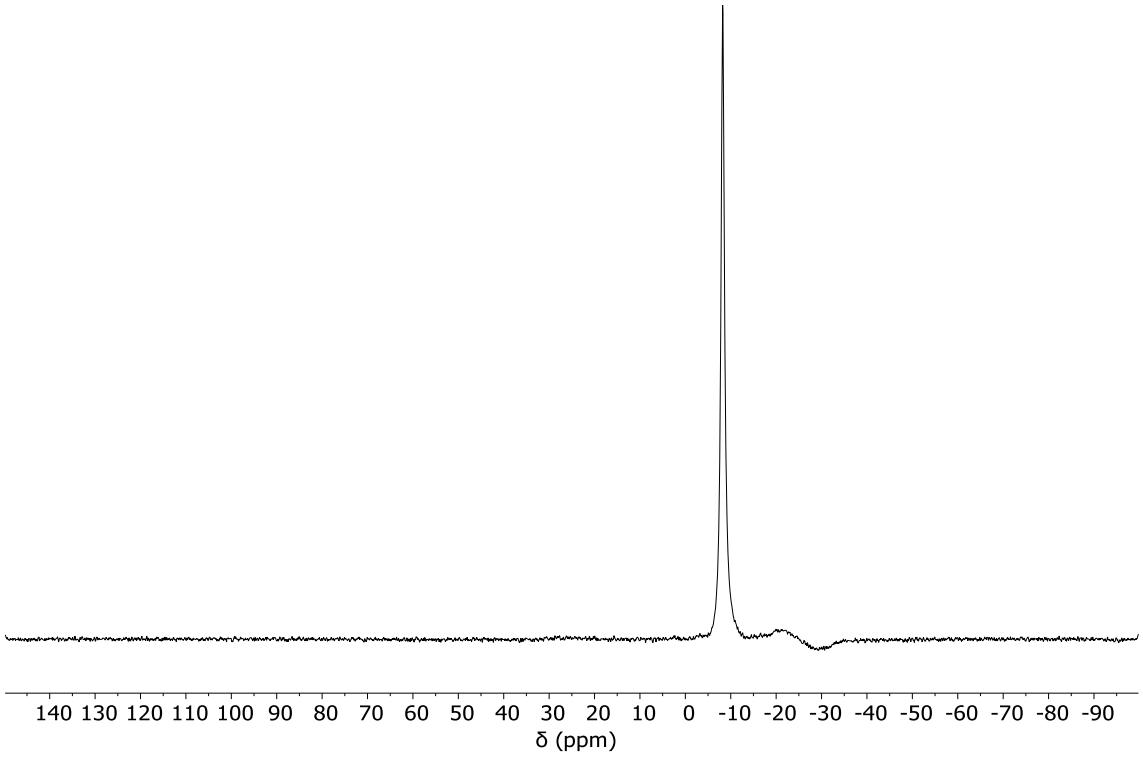

Figure S14. ^{11}B NMR spectrum (THF-d_8, 128 MHz, 298 K) of $[H_2{}^{t\text{Bu,Dipp}}L][H_2N\{B(C_6F_5)_3\}_2]$.

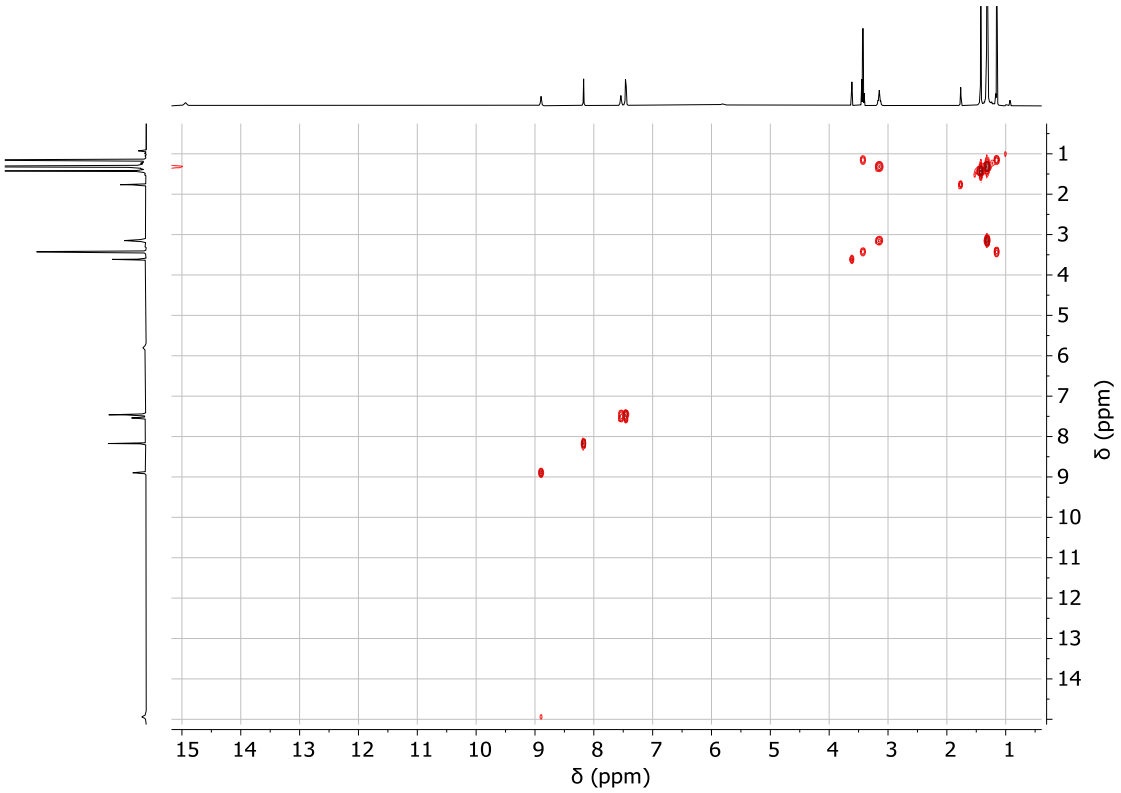

Figure S15. ^{1}H-^{1}H COSY NMR spectrum (600 MHz, THF-d_8, 298K) of [$H_2{}^{t\text{Bu,Dipp}}$L][$H_2N\{B(C_6F_5)_3\}_2$].

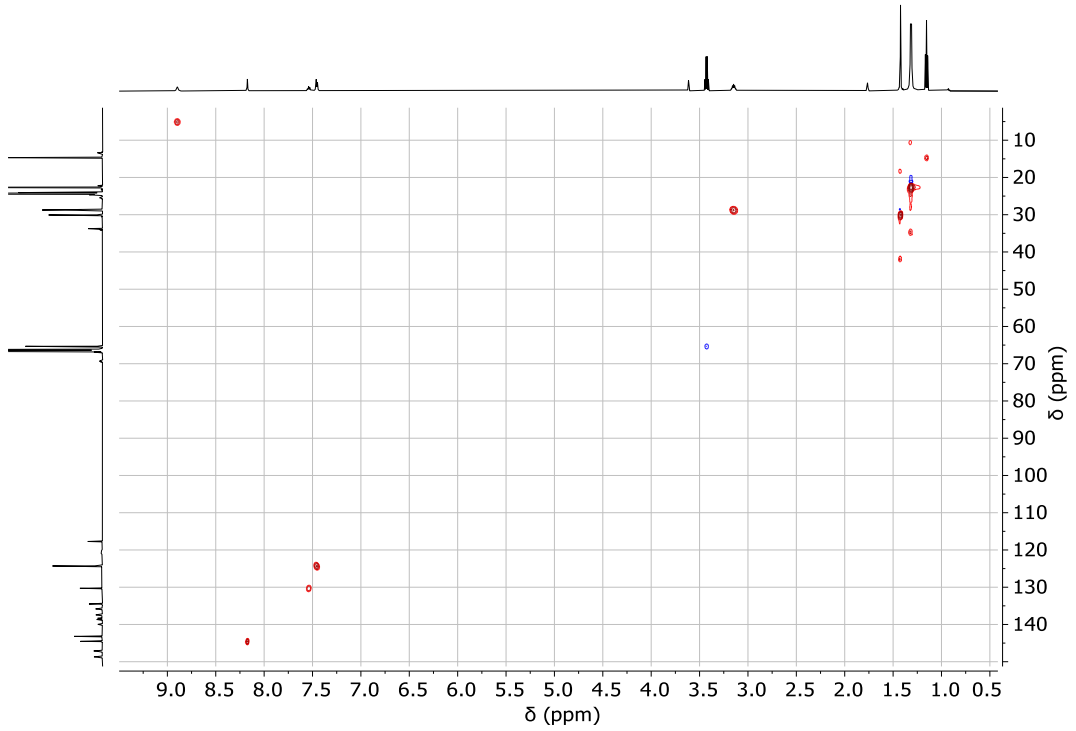

Figure S16. ^{1}H-^{13}C HSQC NMR spectrum (600 MHz, THF-d_8, 298K) of [$H_2{}^{t\text{Bu,Dipp}}$L][$H_2N\{B(C_6F_5)_3\}_2$].

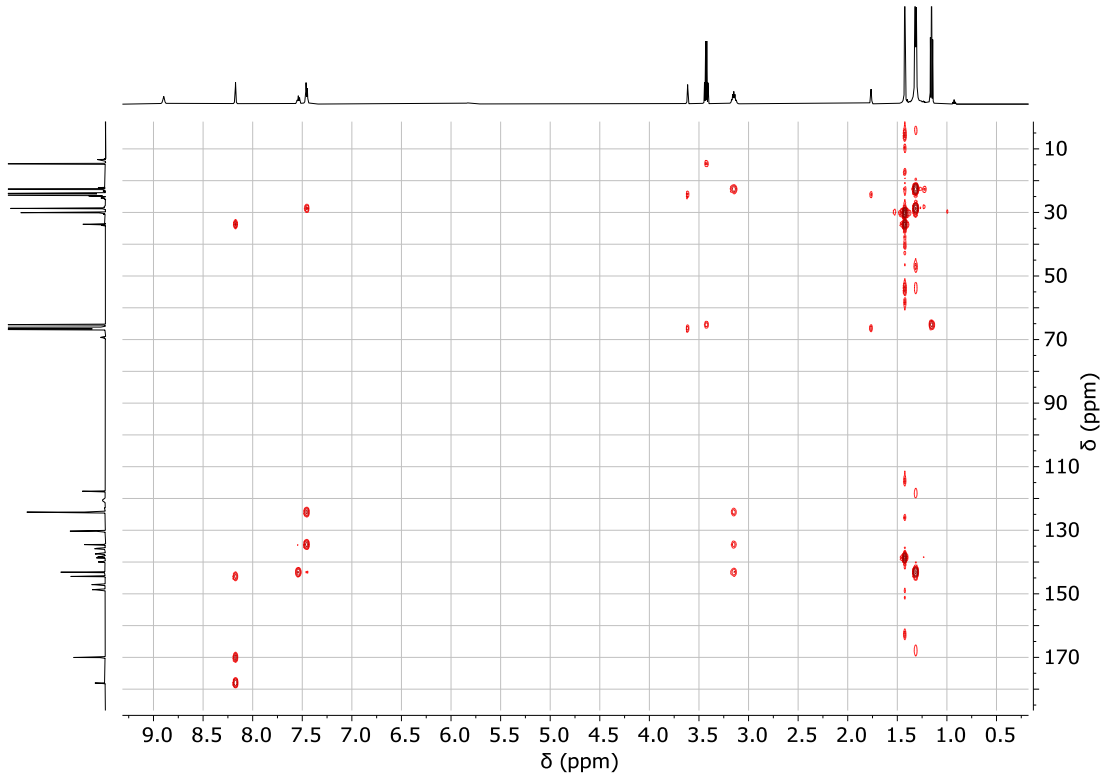

Figure S17. ^{1}H-^{13}C HMBC NMR spectrum (600 MHz, THF-d_8, 298K) of [$H_2{}^{t\text{Bu,Dipp}}$L][$H_2N\{B(C_6F_5)_3\}_2$].

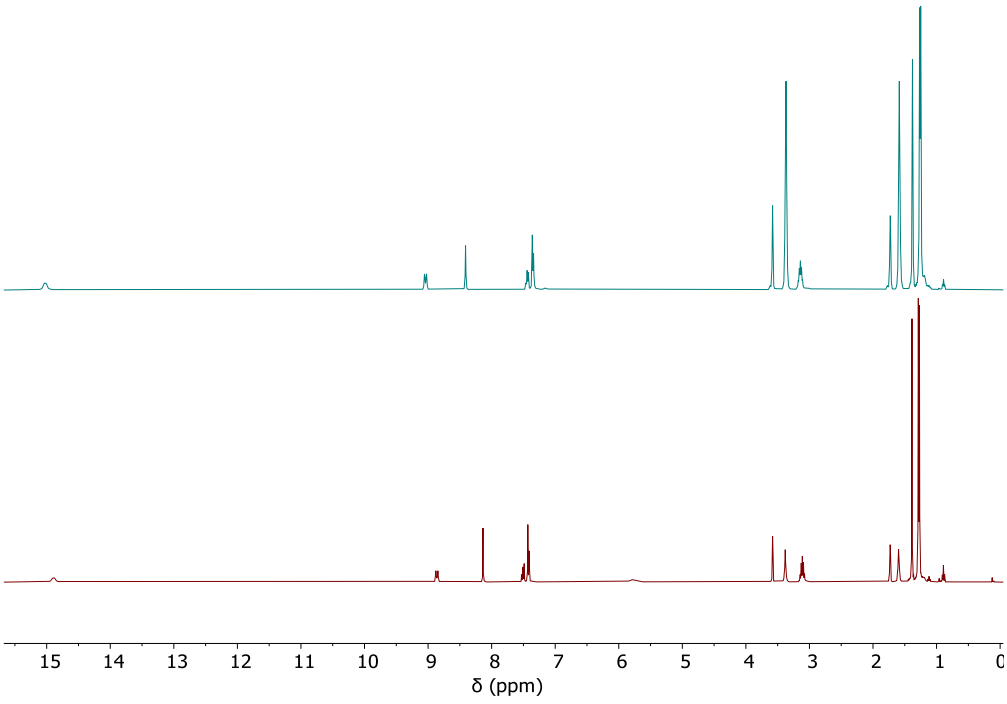

Figure S18. Comparison ^{1}H NMR spectra (400 MHz, THF-d_8, 298 K) of [$H_2{}^{t\text{Bu,Dipp}}$L][BF_4] (blue) and [$H_2{}^{t\text{Bu,Dipp}}$L][$H_2N\{B(C_6F_5)_3\}_2$] (red).

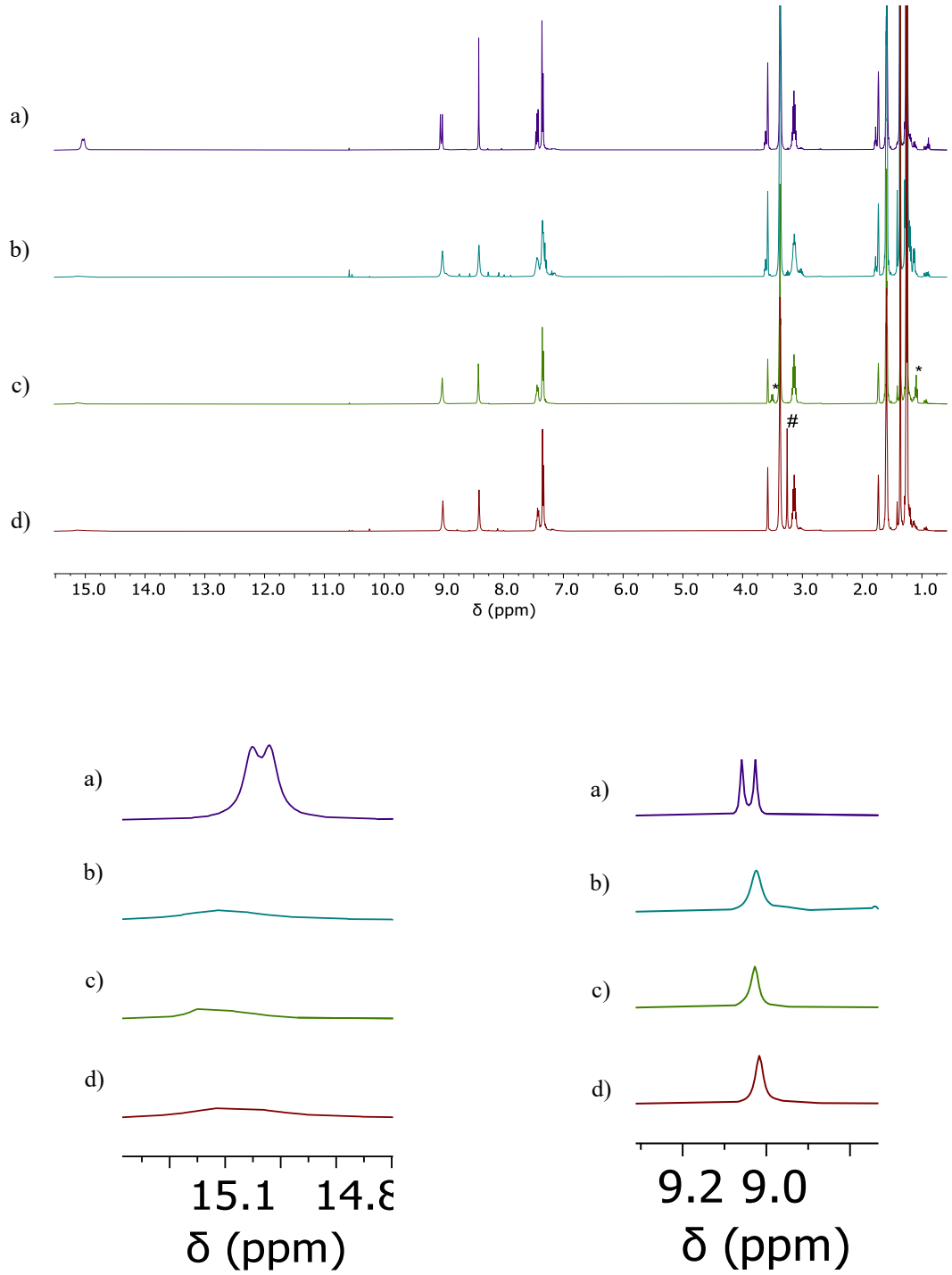

Figure S19. ^{1}H NMR spectra (400 MHz, THF-d_8, 298 K) of [$H_2{}^{t\text{Bu,Dipp}}$L][BF_4] (a)) after treatment with b) water-d_2, c) ethanol-d_1 and d) methanol-d_1. * and # represent protio ethanol and methanol respectively. Expansions highlight difference in N*H* and imine (N=C*H*) resonances upon deuteration.

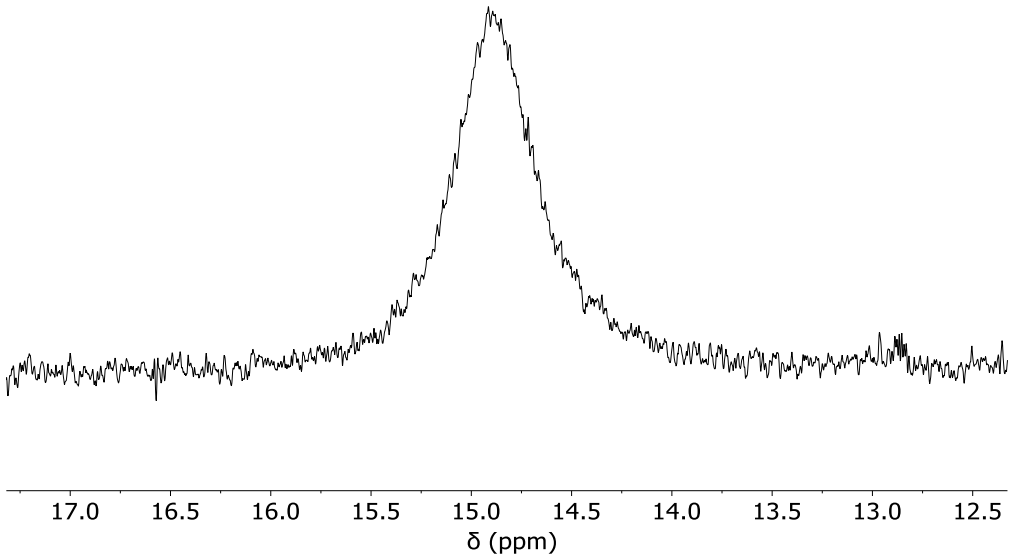

Figure S20. Expanded ^{2}H NMR spectrum (77 MHz, THF-d_8, 298 K) of $[D_2{}^{t\text{Bu,Dipp}}L][BF_4]$ after being deuterated with methanol-d_1.

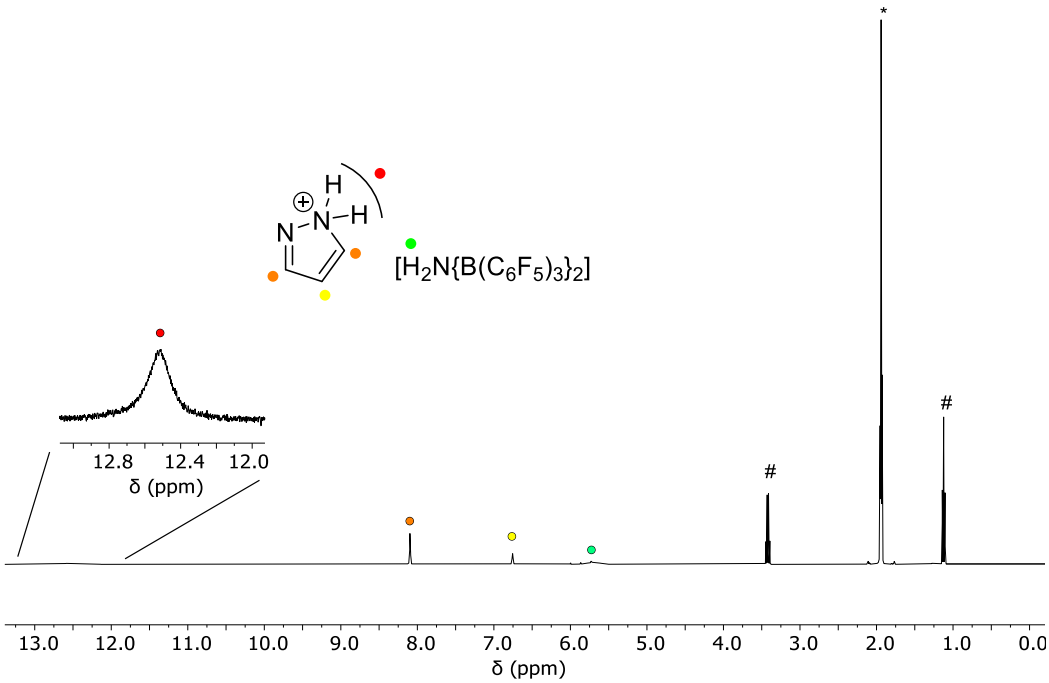

Figure S21. ^{1}H NMR spectrum (acetonitrile-d_3, 400 MHz, 298 K) of [pyrazole-H][$H_2N\{B(C_6F_5)_3\}_2$]. * denotes residual protio solvent fraction of acetonitrile-d_3 and # denotes residual protio diethyl ether.

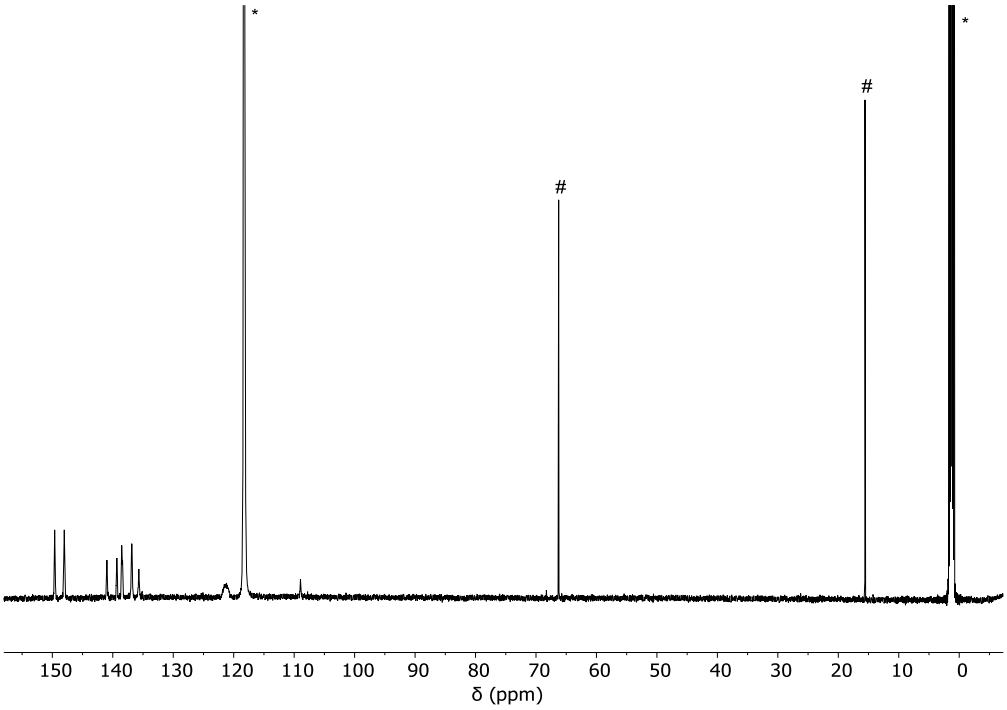

Figure S22. $^{13}C\{^{1}H\}$ NMR spectrum (acetonitrile-d_3, 151 MHz, 298 K) of [pyrazole-H] $[H_2N\{B(C_6F_5)_3\}_2]$. * denotes residual protio solvent fraction of acetonitrile-d_3 and # denotes residual protio diethyl ether.

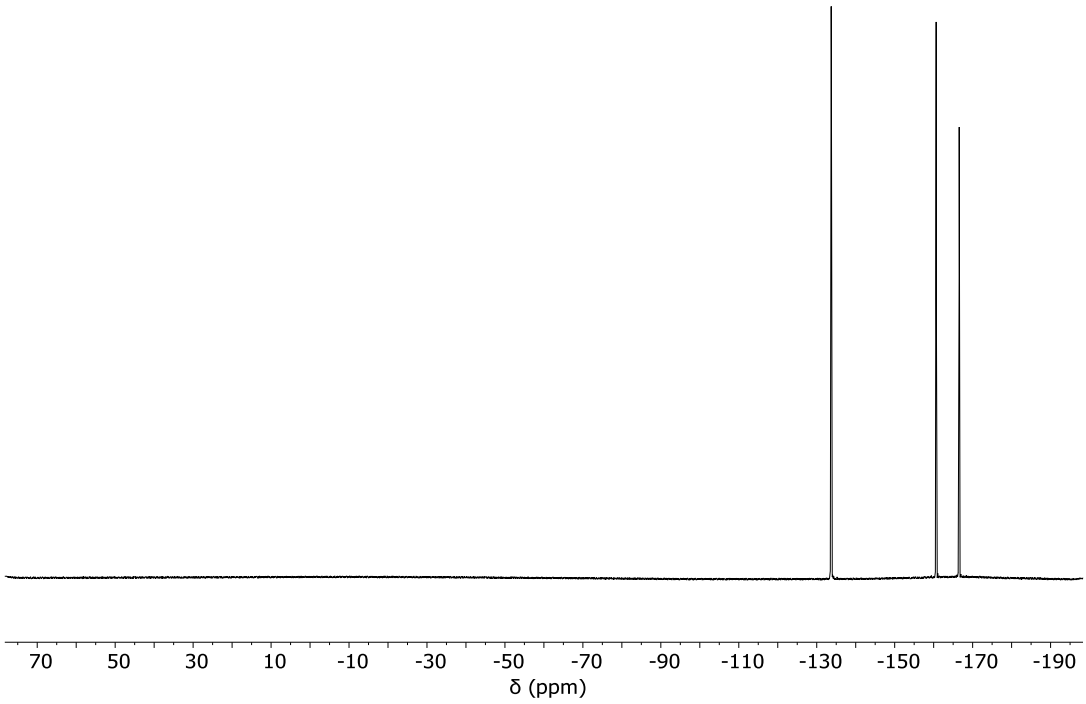

Figure S23. ^{19}F NMR spectrum (acetonitrile-d_3, 377 MHz, 298 K) of [pyrazole-H] $[H_2N\{B(C_6F_5)_3\}_2]$.

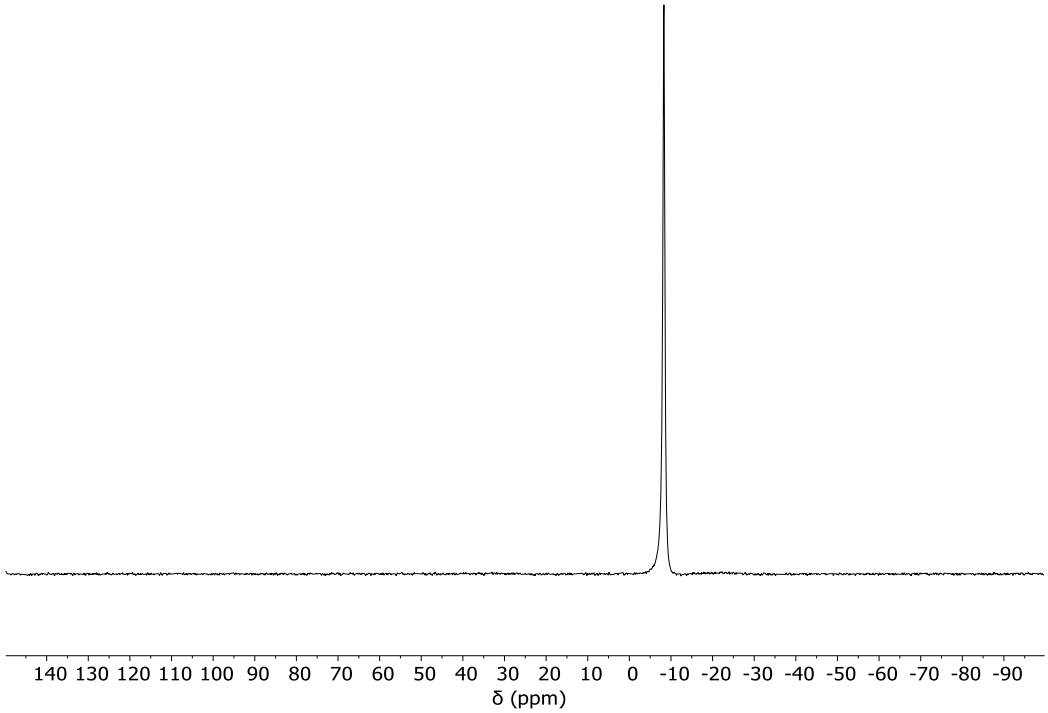

Figure S24. ^{11}B NMR spectrum (acetonitrile-d_3, 128 MHz, 298 K) of [pyrazole-H][$H_2N\{B(C_6F_5)_3\}_2$].

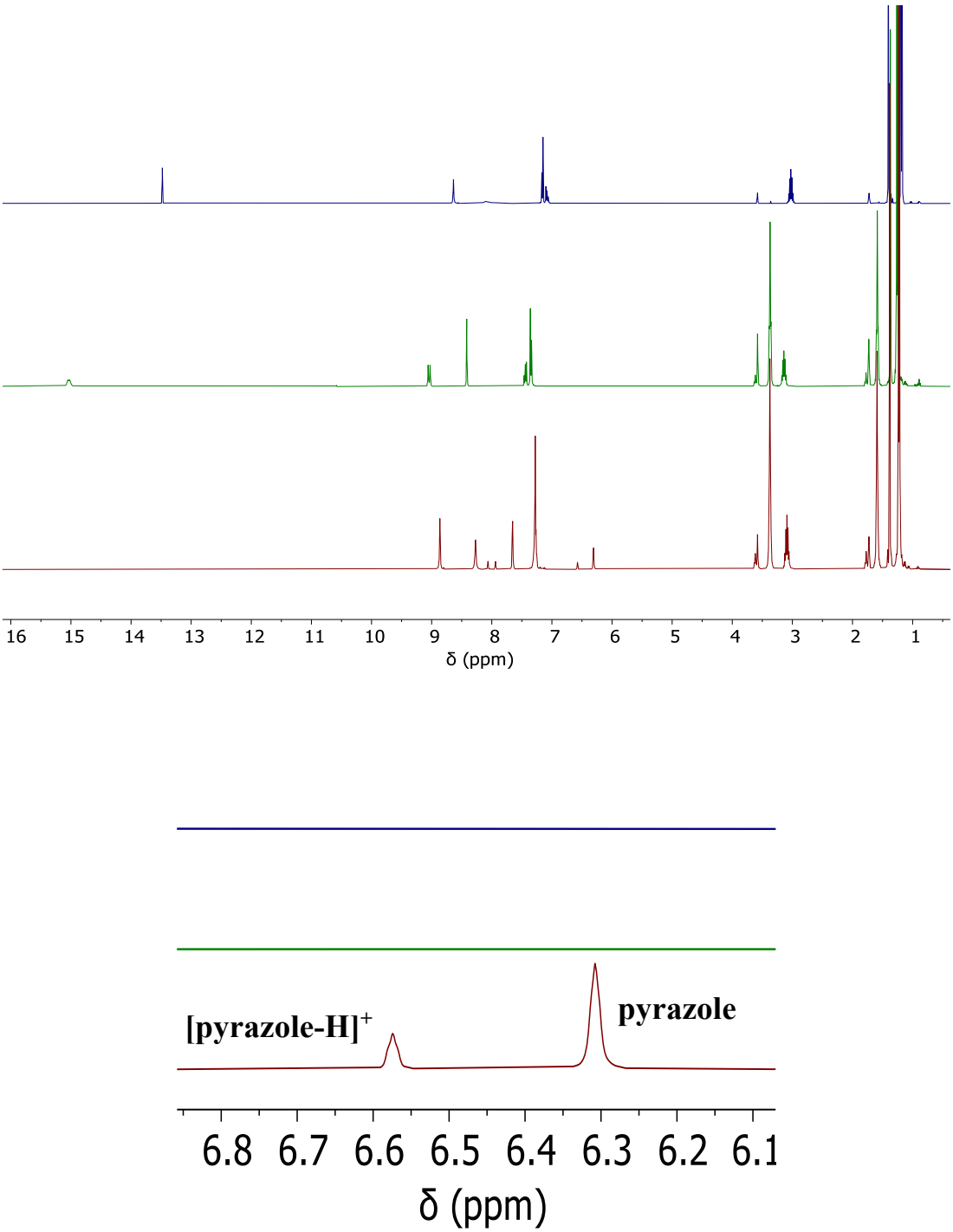

Figure S25. ^{1}H NMR spectra (THF-d_8, 400 MHz, 298 K) of $H_2{}^{t\text{Bu,Dipp}}L$ (blue), $[H_2{}^{t\text{Bu,Dipp}}L][BF_4]$ (green) and 1:1 reaction mixture of $[H_2{}^{t\text{Bu,Dipp}}L][BF_4]$ and pyrazole (red). Expansion highlights signals used in pK_a calculations.

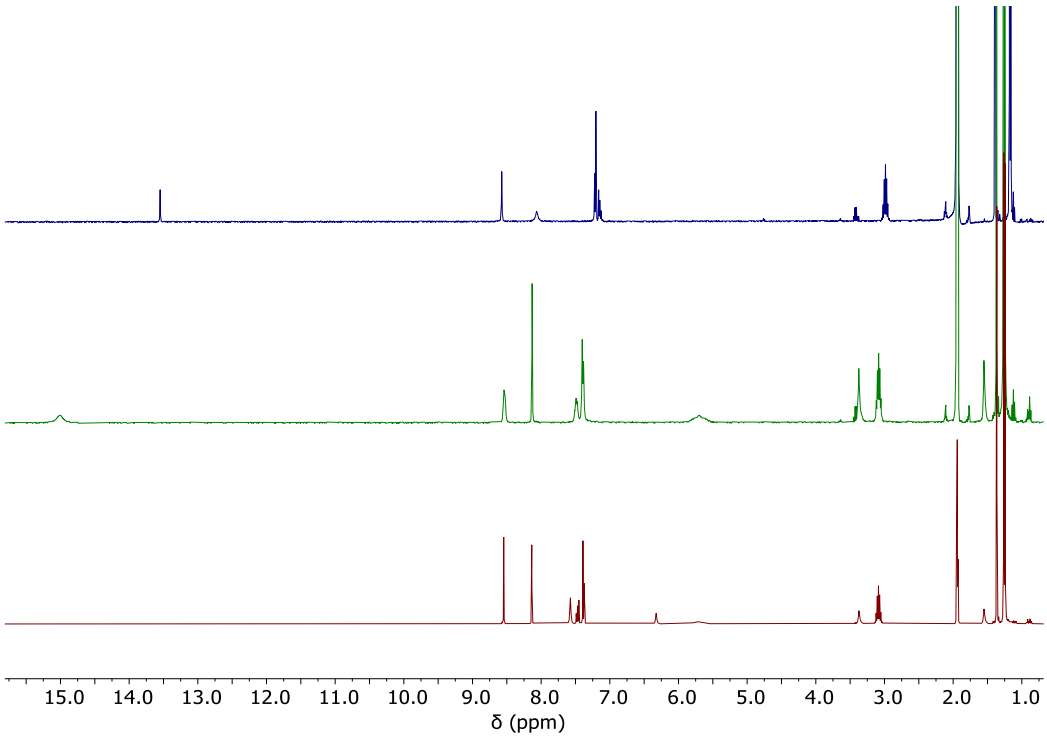

Figure S26. ^{1}H NMR spectra (acetonitrile-d_3, 400 MHz, 298 K) of $H_2{}^{t\text{Bu,Dipp}}L$ (blue), $[H_2{}^{t\text{Bu,Dipp}}L][\ H_2N\{B(C_6F_5)_3\}_2]$ (green) and 1:1 reaction mixture of $[H_2{}^{t\text{Bu,Dipp}}L]$ $[H_2N\{B(C_6F_5)_3\}_2]$ and pyrazole (red).

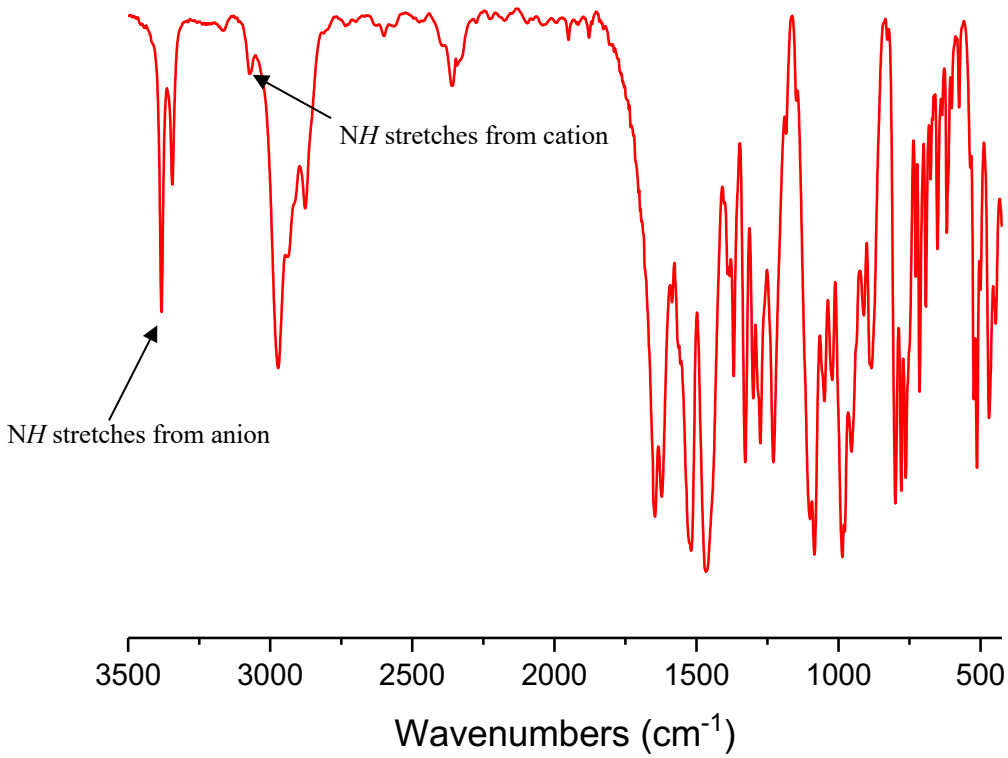

Figure S27. IR (KBr) spectrum of $[H_2{}^{t\text{Bu,Dipp}}L][H_2N\{B(C_6F_5)_3\}_2]$ (**2**).

IV. **Crystallographic data**

Crystals were mounted on MiTeGen MicroMounts using perfluoropolyether oil and rapidly transferred to a goniometer head on a diffractometer fitted with an Oxford Cryosystems Cryostream open-flow nitrogen cooling device.[8] Data collections were carried out at 150 K using an Oxford Diffraction Supernova diffractometer using mirror-monochromated Cu *Kα* radiation (λ = 1.54178 Å) and data were processed using CrysalisPro.[9] The structures were solved using direct methods (SIR-92)[10] or a charge flipping algorithm (SUPERFLIP)[11] and refined by full-matrix least-squares procedures using the Win-GX or CRYSTALS software suites.[12, 13] Where needed, molecular bond lengths and angles were calculated using PLATON.[14] Solid state structural data have been deposited in the Cambridge Crystallographic Data Centre.

Table S1: Selected experimental crystallographic data.

Complex	**$[H_2{}^{t}Bu,DippL][BF_4]$ (1)**	**$[H_2{}^{t}Bu,DippL][H_2N\{B(C_6F_5)_3\}_2]$ (2)**
CCDC number	2235648	2235649
Chemical formula	$C_{36}H_{49}N_2O\cdot 2(C_6H_6)\cdot BF_4$	$C_{73.50}H_{54}B_2Cl_3F_{30}N_3O$
M_r	768.79	1693.18
Crystal system, space group	Monoclinic, $P2_1$	Triclinic, $P\bar{1}$
Temperature (K)	150	150
a, *b*, *c* (Å)	17.0916 (3), 17.0966 (2), 17.6141 (2)	14.6277 (2), 16.6892 (2), 17.0756 (2)
α, *β*, *γ* (°)	90, 118.300 (2), 90	112.6804 (13), 96.2268 (12), 105.7108 (13)
V (Å^3)	4531.80 (13)	3594.61 (10)
Z	4	2
Radiation type	Cu *Kα*	Cu *Kα*
μ (mm^{-1})	0.62	2.29
Crystal size (mm)	0.40 × 0.24 × 0.16	0.23 × 0.18 × 0.13

-- Data Collection --		
Diffractometer	SuperNova, Dual, Cu at zero, Atlas diffractometer	Oxford Diffraction SuperNova
Absorption correction	Gaussian *CrysAlis PRO* 1.171.41.93a (Rigaku Oxford Diffraction, 2020) Numerical absorption correction based on gaussian integration over a multifaceted crystal model Empirical absorption correction using spherical harmonics, implemented in SCALE3 ABSPACK scaling algorithm.	Multi-scan *CrysAlis PRO* (Rigaku Oxford Diffraction, 2017)
T_{min}, T_{max}	0.435, 1.000	0.61, 0.74
No. of measured, independent and observed [$I > 2\sigma(I)$] reflections	51829, 17710, 16472	96321, 14947, 13216
R_{int}	0.030	0.034
-- Refinement --		
$R[F^2 > 2\sigma(F^2)]$, $wR(F^2)$, S	0.050, 0.149, 1.03	0.060, 0.167, 0.99
No. of reflections	17710	14947
No. of parameters	1047	1027
No. of restraints	1	3
$(\Delta/\sigma)_{max}$	< 0.001	0.001
$\Delta\rho_{max}$, $\Delta\rho_{min}$ (e Å^{-3})	0.46, -0.32	1.80, -1.33
Absolute structure	Flack x determined using 6965 quotients [(I+)-(I-)]/[(I+)+(I-)] (Parsons, Flack and Wagner, Acta Cryst. B69 (2013) 249-259).	-
Absolute structure parameter	-0.24 (7)	-

Computer programs: *CrysAlis PRO* 1.171.41.93a (Rigaku Oxford Diffraction, 2020); *SUPERFLIP* (Palatinus and Chapuis, 2007)[11]; *SHELXL2018*/3 (Sheldrick, 2018); *SUPERNOVA* (Oxford Diffraction, 2010), *ORTEP-3 for Windows* (Farrugia, 1997)[15]fa, *CRYSTALS* (Betteridge *et al.*, 2003) and *CAMERON* (Watkin *et al.*, 1996).

Table S2: Experimental metrical parameters for the O2-containing cationic fragment present in the asymmetric unit of **1** (bond lengths given in Å).

C(37)-O(2)	1.276(3)
C(37)-C(38)	1.441(3)
C(37)-C(42)	1.431(3)
C(38)-C(43)	1.422(3)
C(42)-C(56)	1.418(3)
N(3)-C(43)	1.299(3)
N(4)-C(56)	1.301(3)
N(3)-H(3A)	0.90(4)
N(4)-H(4)	0.91(4)

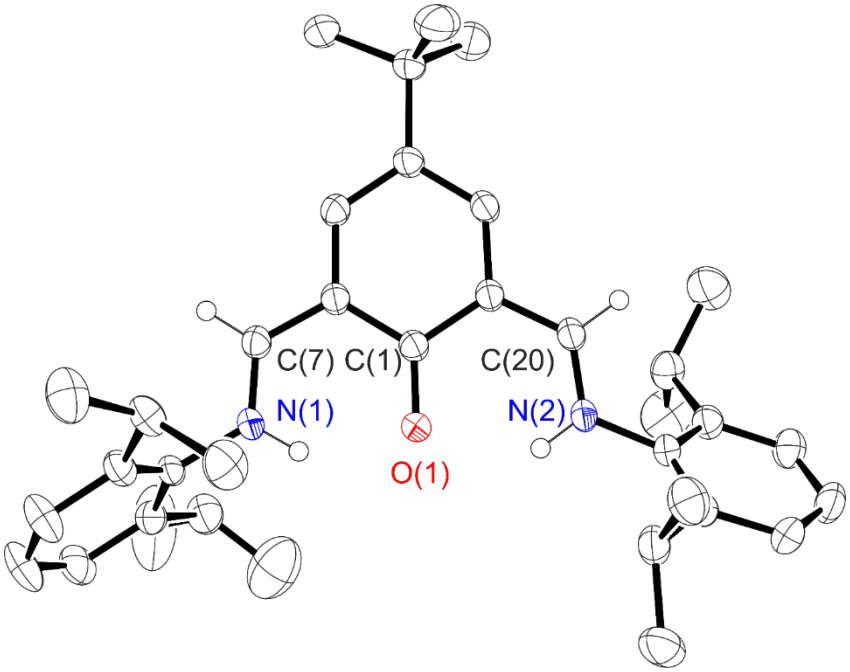

Figure S28. Thermal displacement ellipsoid drawings (30% probability) of $[H_2{}^{t\text{Bu,Dipp}}L][H_2N\{B(C_6F_5)_3\}_2]$; cation only displayed. All hydrogen atoms apart from those on N1, N2, C7 and C20 have been omitted for clarity.

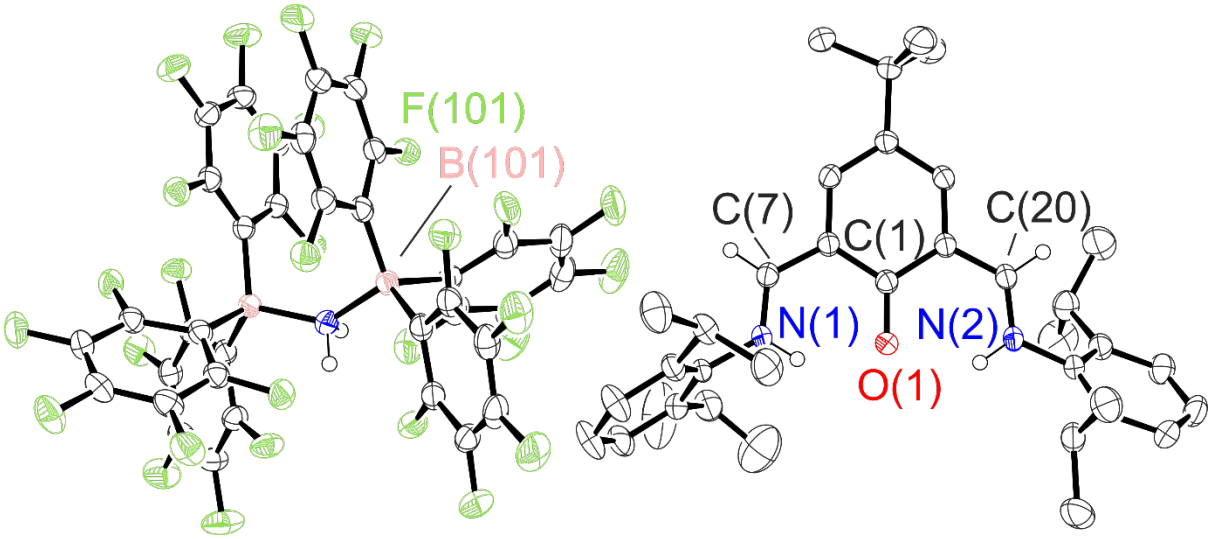

Figure S29. Thermal displacement ellipsoid drawings (30% probability) of $[H_2{}^{t\text{Bu,Dipp}}L][H_2N\{B(C_6F_5)_3\}_2]$. All hydrogen atoms apart from those on N1, N2, C7 and C20 have been omitted for clarity.

V. Density functional theory details

All density functional theory (DFT) calculations were performed with the ORCA 5.0.3 software package.[16-18] Geometry optimisations were carried out at the B3LYP[19-21] level of theory using the def2-TZVP basis set reported by Neese *et al.* (segmented all-electron relativistic basis sets, SARC).[22, 23] Analytical frequency calculations were carried out to verify all geometries were true minima (NIMAG = 0). Single point energy calculations on all compounds were performed with and without Grimme's DFT-D3 dispersion corrections.[24] The Resolution of Identity approximation (RIJCOSX) was used to accelerate the calculations.[25, 26] Molecular orbitals maps were generated with the program Chimera[27] and contour plots of (Laplacian) electron density were produced and analysed using Multiwfn 3.8.[28]

Representative input file:

```
#geometry optimization and frequency calculation of [H2tBu,DippL][BF4]

!RKS B3LYP D3ZERO RIJCOSX SlowConv TightSCF def2-TZVP Normalprint Opt Freq
PAL8

%maxcore 2000

!CPCM(THF)

*xyz +1 1

[INSERT CARTESIAN COORDINATES HERE]
```

Table S3: Calculated delocalisation indices – δ(A,B) – reported in atomic units

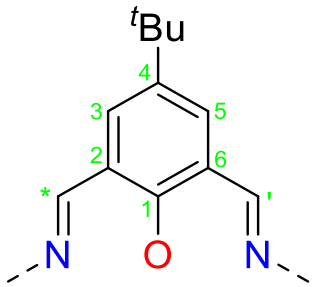

	$H^{tBu,Dipp}L$	$[HN<O>NH]^+$	$[N<OH>NH]^+$	$[N<OH_2>N]^+$
(L)N-H	-	0.63	0.66	-
N=C*	1.53	1.28	1.31	1.54
C*-C2	1.05	1.21	1.17	1.03
C2-C1	1.28	1.11	1.20	1.32
C2-C3	1.31	1.29	1.28	1.31
C3-C4	1.38	1.37	1.37	1.36
C4-C5	1.38	1.34	1.34	1.34
C5-C6	1.34	1.31	1.33	1.32
C6-C1	1.25	1.10	1.23	1.31
C-O	0.95	1.19	1.00	0.75
O-H	0.59	-	0.42	0.47
				0.48
C6-C’	1.05	1.19	1.08	1.02
C’=N	1.52	1.30	1.47	1.54
N-H (R)	-	0.63	-	-
$\frac{1}{2}\sum_{A\neq B}\delta(A,B)$	7.32	7.48	7.43	7.40
Difference	-	+0.16	+0.11	+0.08

Table S4: Final single point energies of dispersion corrected, optimised structures

Structure	Single point energy (with DFT-D3; kJ/mol)	Dispersion correction (kJ/mol)
$H^{tBu,Dipp}L$	-4161753.1	-263.0
$[HN<O>NH]^+$	-4163011.8	-271.2
$[HN<OH>N]^+$	-4162985.1	-270.1
$[N<OH_2>N]^+$	-4162736.5	-274.1

Table S5: Thermodynamic parameters of dispersion corrected, optimised structures

Structure	ΔG (kJ/mol)	ΔH (kJ/mol)	ΔS (kJ/mol)
$H^{tBu,Dipp}L$	-4159940.4	-4159657.2	-283.3
$[HN<O>NH]^+$	-4161155.8	-4160872.7	-283.0
$[HN<OH>N]^+$	-4161133.2	-4160849.6	-283.6
$[N<OH_2>N]^+$	-4160892.7	-4160603.2	-289.4

Cartesian coordinates of dispersion corrected, optimised structures

$H^{tBu,Dipp}L$

C	0.78314396810748	2.88273995236313	4.72990545357103
C	0.85235658810653	2.78046550772180	3.33132925838298
C	-0.32680854752067	2.56093882067278	2.60541483743456
H	-0.22182935236235	2.47884717035954	1.53407895559077
C	-1.56847045138657	2.42894662008805	3.21255054127454
C	-1.60080939999813	2.52433448388487	4.60476000009606
H	-2.53669421554682	2.42356855712700	5.13737969152423
C	-0.46061450364909	2.74450116410775	5.37552651813946
C	2.13469839170745	2.84678400436980	2.62371800086334
H	3.04715595998715	2.70076610500677	3.21545800661719
C	3.47050490433212	2.99171874455455	0.71909638643894
C	3.94187251605101	1.76456228953801	0.20589905395269
C	5.13911582734877	1.77214603027937	-0.50933001424777
H	5.52918584203303	0.84652185719655	-0.91020161409764
C	5.84832423148491	2.94861474244051	-0.71553528629796

H	6.77699883828471	2.93112656809053	-1.27305599976457
C	5.36678075044670	4.14611360785818	-0.20369022722971
H	5.93124308235667	5.05398553776501	-0.36885347492781
C	4.17479621289453	4.19611062648471	0.51960478191811
C	3.12902935118691	0.49029769881195	0.39748539879999
H	2.73983030415459	0.49797285020955	1.41887121373008
C	1.91632666298190	0.47932425994822	-0.55076122175821
H	1.29503419581582	1.36324540622344	-0.40510539626035
H	1.30058956796794	-0.40582021532841	-0.37328951738990
H	2.25016728248011	0.46045615594383	-1.59157600993192
C	3.93930091698467	-0.79910349029871	0.24112443716811
H	4.27235831494033	-0.94608108049593	-0.78903859315218
H	3.31787882542008	-1.65632468612623	0.50825118931991
H	4.82039388199688	-0.80297008465170	0.88635367820191
C	3.60801192987295	5.51064169416647	1.03795734611807
H	3.13867101340523	5.31080680045534	2.00398192314028
C	2.50722461112792	6.02181617059209	0.09140745434963
H	2.93045374579234	6.25187483464883	-0.88995663045807
H	2.05079030635254	6.93223208962916	0.48776683029301
H	1.72317025678397	5.27494646851304	-0.04092060633599
C	4.66204733930265	6.59638429188105	1.27212545094311
H	5.47083849653855	6.23804108309468	1.91251590928078

H	4.19986770232312	7.45892625757907	1.75678066569633
H	5.10059512403524	6.94525919860035	0.33452244244813
C	-0.54422073807702	2.82274357180277	6.83918219785038
H	0.39799095891578	2.95515736668685	7.37433680934429
C	-1.67268325452522	2.81662114248768	8.87460074804120
C	-2.01462729684432	1.64910120572884	9.59319693767122
C	-2.07747727522487	1.71781846844642	10.98166931309353
H	-2.32258066892850	0.83123130790435	11.55186578767507
C	-1.82634103935651	2.90984644120531	11.65348741747334
H	-1.87641399484205	2.94527930434657	12.73508513161787
C	-1.52228235837961	4.05397594555109	10.93212466799355
H	-1.34050691450047	4.98177263570518	11.46082957116724
C	-1.44439614425503	4.03919995415398	9.53689854226577
C	-2.24268597789925	0.34654298109707	8.84451735309961
H	-2.63739705778203	0.61334255028518	7.86007931961203
C	-3.25951494433033	-0.58396120733927	9.51381754960195
H	-2.88235247210629	-0.98896915609041	10.45569170048961
H	-3.47284594776806	-1.43080495273578	8.85789689287875
H	-4.19862886968491	-0.06604997328702	9.71947546509241
C	-0.90924814741543	-0.38628013211792	8.61605761422577
H	-0.19249255625725	0.24667622100703	8.09002293348387
H	-1.06412041630795	-1.29162717874377	8.02364197783960

H	-0.46599635885308	-0.67566638273988	9.57261085309510
C	-1.14056082419434	5.33068038710181	8.79015184927214
H	-1.26236462343783	5.14485998784663	7.72323562588662
C	-2.12381523478630	6.45230118890082	9.15910836339345
H	-3.15648516179985	6.13832083503735	8.99322686377762
H	-1.93251831785830	7.33604338179638	8.54570880312511
H	-2.02372098589299	6.74703365369821	10.20595131922604
C	0.31107707676634	5.78017132450923	9.01651802618240
H	0.49215214004215	5.98806403402946	10.07400085327687
H	0.52252200481148	6.69147689092145	8.45151919607578
H	1.01688393004805	5.00956059332150	8.69984217387017
C	-2.86236786750997	2.17743973894633	2.42826574303569
C	-2.61008700020670	2.05540759352515	0.91844660170611
H	-2.18235700268951	2.97121817855031	0.50467389528185
H	-3.55614817805791	1.86910568055969	0.40657783863090
H	-1.93652010570188	1.22715186117785	0.68788325883877
C	-3.83480572394103	3.35126821351723	2.66688980036055
H	-4.08305039125387	3.45863595237723	3.72417658747303
H	-4.76488513856577	3.18540871085885	2.11784034593326
H	-3.39663151574189	4.29111517330592	2.32333084500742
C	-3.51201683583611	0.86689640213185	2.91810309890135
H	-2.83946725250066	0.02037880916812	2.76146558511609

H	-4.43570441600722	0.67663643653219	2.36614737502474
H	-3.76002333288943	0.91151437344418	3.97964510798380
N	2.21625337321584	3.02156156930973	1.36827336138983
N	-1.64755507883299	2.72973410332920	7.46583567217747
O	1.86642135539140	3.11687153302862	5.51951535281880
H	2.65467610971057	3.31757018641510	5.00082083918033

[HN<O>NH]$^{+}$

H	-5.64896554864746	-0.39559521610841	2.01214807359579
H	-2.09870212578406	-0.14559891255122	2.27238122815624
C	-3.77057461845199	-1.95784333323839	2.29001231711053
C	-2.50489656598537	-2.64386720346748	2.45087137123237
C	-2.45829291592527	-4.03840403057095	2.56636016809846
H	-1.48066888834947	-4.49044602365252	2.68813240456402
C	-3.58957505488974	-4.85461925820707	2.52717753727677
C	-4.80858543687345	-4.20972192978859	2.35620200326632
H	-5.72223074111414	-4.78820065019561	2.30998421596886
C	-4.93563848246758	-2.81401954609293	2.24001086637853
C	-1.28468302370500	-1.92290029799071	2.48809580350389
H	-0.35355178782966	-2.46643697496911	2.61520920585374
C	0.03394447387594	0.11377350987903	2.38358920996019
C	0.30752278561789	0.89758404625524	3.51333014159568

C	1.49937846391518	1.62161648230500	3.51655656927455
H	1.75563113756417	2.23170797112449	4.37163455933398
C	2.36770307522455	1.56371257529368	2.43572756427883
H	3.29070569525532	2.13017102955053	2.45645291077300
C	2.06120718642609	0.78969404736165	1.32408467926252
H	2.74847419977975	0.77277384196109	0.49021586096412
C	0.88151640926903	0.04720351521256	1.26520862382682
C	-0.63172542471679	0.89848814500095	4.70951383203639
H	-1.64842052460929	0.74431542461106	4.33904404863676
C	-0.29806662669785	-0.27797814169944	5.64373587884641
H	-0.34371764018695	-1.23459934953566	5.12000797573653
H	-1.00155115239354	-0.31316767748001	6.47845375389196
H	0.71028109909234	-0.16466148064260	6.04905963443811
C	-0.63735198135915	2.22048194125620	5.48410518387872
H	0.30884517592269	2.39115885107565	6.00133713100392
H	-1.42379104728995	2.19713140856078	6.24080532818167
H	-0.82319561427330	3.06911716494427	4.82307180186810
C	0.49103686568054	-0.72984825473576	0.01449122513551
H	0.01816616669542	-1.66462966572826	0.32301094758449
C	1.67815606151599	-1.11890556687857	-0.87105659129958
H	2.13882296245051	-0.24615708193962	-1.33836427357441
H	1.33309806691780	-1.77482348505339	-1.67226261066067

H	2.44588896399632	-1.64807115804827	-0.30330791486539
C	-0.54899711039106	0.06598325950209	-0.79442202089945
H	-1.43547496475930	0.29352626589225	-0.19979124363465
H	-0.86470414164863	-0.50433565323354	-1.67066783607684
H	-0.11908971304789	1.01050274319989	-1.13652710457203
C	-6.22954912356931	-2.27090208108636	2.05523283922888
H	-7.07306517954406	-2.94606084730277	1.96454369655583
C	-7.77145385729539	-0.41359360146798	1.74863290893580
C	-8.83779360309198	-0.70749198743411	2.61274323587163
C	-10.08144404047590	-0.15214872695923	2.29853063157800
H	-10.93055089982520	-0.36417143499077	2.93524596725389
C	-10.24387464907519	0.67734583665545	1.20199852098097
H	-11.21839856553237	1.09476266367362	0.98034749822618
C	-9.15671332671896	0.99190697621970	0.39369602547096
H	-9.29938413021133	1.65455453981820	-0.44819472314844
C	-7.89791537643649	0.45728785925991	0.64762952276315
C	-8.70012472160144	-1.54231158702239	3.87850522744784
H	-7.65072990924260	-1.80009949792243	4.02157345818531
C	-9.49430707211475	-2.85371163267794	3.77955338722567
H	-10.56336945834910	-2.65310629282398	3.68084656052151
H	-9.34473589327540	-3.45353435915406	4.67973050208965
H	-9.18625550874225	-3.44830858682442	2.91693534762800

C	-9.11833576795361	-0.74068424844012	5.12191659272684
H	-10.17973261435928	-0.48706869075696	5.09677598987828
H	-8.54809250704989	0.18692525932877	5.19991346279615
H	-8.93733738902448	-1.33184801202187	6.02223673958792
C	-6.71150727642992	0.74373845561355	-0.26297457314072
H	-5.81227456216652	0.79572566214836	0.35687291260030
C	-6.51524615614624	-0.40589300657033	-1.26775032463089
H	-6.39058077407948	-1.36693729643183	-0.76665642928936
H	-5.62988626305588	-0.22534778467328	-1.88103625381862
H	-7.38209922340652	-0.47793563806118	-1.92883479658502
C	-6.80840673010122	2.08512312413196	-0.99624386649054
H	-7.60737889558074	2.08167972895322	-1.74039097024964
H	-5.87228341627247	2.28054005497042	-1.52232108118784
H	-6.99002524347503	2.90865103707578	-0.30314865921063
C	-3.44705482336101	-6.37610117905191	2.66403798830691
C	-2.78395483125209	-6.70547465429678	4.01737423715214
H	-2.67420443166083	-7.78681745499788	4.12570339847133
H	-3.39303509256847	-6.33800166419179	4.84627393940381
H	-1.79106517532627	-6.26022383512819	4.10121557758872
C	-2.56528331779091	-6.91029776083996	1.51635844680504
H	-3.01808694664099	-6.69203487826460	0.54659317223750
H	-2.45125017343711	-7.99297176293007	1.60531061816193

H	-1.56769842286581	-6.46794598434111	1.53312859509761
C	-4.80476996161450	-7.08998551581280	2.60521554937021
H	-5.31239012276232	-6.91971615562165	1.65299613659673
H	-5.46674331155164	-6.76832111862460	3.41248212736977
H	-4.65187859247498	-8.16532419751159	2.71068335118835
N	-1.19737298545438	-0.62889624345446	2.37364967935268
N	-6.48271825084532	-0.99322032444510	1.96637872839895
O	-3.84827008399263	-0.69760148689261	2.19144564476632

[N<OH>NH]$^{+}$

H	-2.15619787465930	-0.11922254043315	2.23366712469819
C	-3.86778041782845	-2.06808298383007	2.37960900393509
C	-2.60954904080428	-2.64095844094987	2.68465895821366
C	-2.52954180398630	-4.02134324178383	2.95025657294143
H	-1.55135144722146	-4.42596964296113	3.17670168463362
C	-3.63604588503372	-4.85984382183475	2.92517956778667
C	-4.86187490900218	-4.26782672394955	2.60805980206875
H	-5.75866096091708	-4.87110885532609	2.56085004436934
C	-5.00261089338619	-2.90378945684644	2.33775626099970
C	-1.40024860062022	-1.88644578336133	2.70627036397995
H	-0.47624979001074	-2.41004186599804	2.92777938538906
C	-0.06800220647821	0.13356292339591	2.48463651745283

C	0.65739469436228	0.25552041732554	3.67827721166891
C	1.83988286718084	0.99848817979258	3.62314362083440
H	2.43449211456238	1.11306500596886	4.51999739038321
C	2.25800390221034	1.59990027479473	2.44743956578849
H	3.17684400772874	2.17302806038132	2.43270568699964
C	1.50387412379622	1.47501811139301	1.28617134284828
H	1.84697082368488	1.95125828930470	0.37822776364355
C	0.32457298691874	0.73617025119500	1.27561903934714
C	0.21177095974566	-0.33930629772542	5.00581947003731
H	-0.76335525176006	-0.80816768906911	4.87574288442017
C	1.18583302481873	-1.42614655243155	5.48595549159367
H	1.29578730483354	-2.21885806209641	4.74286505522669
H	0.82285682809479	-1.87325410330531	6.41364697113482
H	2.17534671985911	-1.00621059449568	5.67827492442713
C	0.02927930738044	0.75146015232365	6.07294980632973
H	0.97604279861974	1.24071911109948	6.30906138683739
H	-0.35775355013822	0.30872720432111	6.99311914335544
H	-0.67452503435119	1.51525216632011	5.73673128909764
C	-0.51842137079361	0.59957986049017	0.01605006032760
H	-1.06677803282796	-0.34326088397154	0.08201749619745
C	0.31431948099404	0.53508616479351	-1.26970952173838
H	0.80722811444198	1.48579901474185	-1.48128080556687

H	-0.33828792481062	0.31030047608734	-2.11536858977259
H	1.07915902371450	-0.24147621859829	-1.21080015247608
C	-1.55197212450129	1.73758112725910	-0.06956490030459
H	-2.19387381142120	1.78011554086957	0.81301098699367
H	-2.19080562630663	1.60178128316429	-0.94479259500585
H	-1.04544316531570	2.70135136287491	-0.16012578894175
C	-6.29768174426441	-2.34953684800927	1.97434218956346
H	-7.14227861921696	-3.03821577192849	1.90953944083093
C	-7.65652133134284	-0.52031535447614	1.33300345479496
C	-8.77290271468000	-0.53637034834322	2.19125324189094
C	-9.94747776047756	0.06940602005886	1.73595272462048
H	-10.82349404672283	0.06700605576072	2.37236384943191
C	-10.01411055317227	0.67749233087644	0.49305444405340
H	-10.93847988005518	1.13451332094086	0.16158902302943
C	-8.88898217506855	0.71313548578077	-0.32377311779497
H	-8.95121937452043	1.20043610592825	-1.28727505634727
C	-7.69191321720148	0.13071905284168	0.07961217533635
C	-8.74546037202482	-1.13685200190061	3.59005349386973
H	-7.72635389309347	-1.45051673566424	3.81527867523177
C	-9.64470123154701	-2.37910956690675	3.68620384961524
H	-10.68724227302965	-2.11945303748471	3.48887149249259
H	-9.58841664668573	-2.81316560968662	4.68714646074786

H	-9.34724589818330	-3.14268072387471	2.96448752773580
C	-9.12927272482071	-0.10076314409756	4.65862574237774
H	-10.16497279836448	0.22588722374089	4.54739441090270
H	-8.48796110925213	0.78091243844940	4.59878371938753
H	-9.02288246134646	-0.53523635116997	5.65521140648239
C	-6.46903408650978	0.11773806221502	-0.82466929165585
H	-5.58691534995366	0.13478887113761	-0.18050379410202
C	-6.41686478178770	-1.18873813390193	-1.63622176761771
H	-6.43268692518017	-2.06414835127527	-0.98490925854421
H	-5.50738380355566	-1.22883142234878	-2.24046978689106
H	-7.27664346605246	-1.25066559079683	-2.30798491932096
C	-6.37047850870484	1.33217644875674	-1.75311381706128
H	-7.14895145444042	1.32169786194787	-2.51884396779677
H	-5.40699621184836	1.32352210439162	-2.26687912270325
H	-6.45300297668094	2.26782259129281	-1.19657714617249
C	-3.47493263524685	-6.35772785909751	3.21822199459735
C	-2.85758784072664	-6.54242950409594	4.61987342202754
H	-2.73698017750823	-7.60647478258603	4.83414955162042
H	-3.50215360711449	-6.10909652395870	5.38780809243100
H	-1.87463543894048	-6.07491142877766	4.69539662480220
C	-2.54107360954859	-6.98042979942060	2.15954583360495
H	-2.95976662274785	-6.86447997250872	1.15748896496597

H	-2.41396212144948	-8.04706535929527	2.35693960134761
H	-1.55253015256448	-6.51806186411899	2.17156336996997
C	-4.81777919071337	-7.10081587621195	3.17948989139515
H	-5.28856454229238	-7.03840912989261	2.19594840251130
H	-5.51678549418860	-6.71210509589419	3.92350115890382
H	-4.65133276413697	-8.15645618779211	3.39994171970412
N	-1.29636411344956	-0.61416679067922	2.46659590703158
N	-6.42199650617399	-1.10262391741741	1.70971120376801
O	-3.96181633276573	-0.76645596197200	2.12463760690024
H	-4.95843982141936	-0.58338614746427	1.90446085787635

[N<OH_2>N]$^+$

C	-2.89896747059358	-3.88328403979916	2.46151490998146
C	-1.55849445965881	-3.81090901857204	2.80883319269676
C	-0.94155374591510	-5.02155535362729	3.13024759812984
H	0.10161434062481	-4.97702103790707	3.40847847614445
C	-1.61963640469298	-6.24267628496022	3.09655146114297
C	-2.96381424843560	-6.23251132007765	2.73215424691876
H	-3.54089475467018	-7.14330079401345	2.69709142223441
C	-3.64287466635098	-5.05006166443495	2.41150041303765
C	-0.81952453216432	-2.53660932014624	2.83134002566058
H	-1.33701274790518	-1.65584990407855	2.44753652071168

C	1.04481331707716	-1.23047590316941	3.28873820623848
C	0.61881081780087	-0.17398743558356	4.11845131146166
C	1.35916193621802	1.01111714683825	4.09157676723331
H	1.05043131372021	1.83964232875063	4.71690078689853
C	2.47884749996246	1.14891427886441	3.28653981545643
H	3.03067563065600	2.08093731885492	3.27900093747278
C	2.90067223413199	0.08311702916536	2.49832958973301
H	3.78157004777568	0.19729206423992	1.88072010182635
C	2.20679247766989	-1.12267791804556	2.49344472646384
C	-0.57243824079325	-0.28527418456557	5.06092142297768
H	-0.93346661290306	-1.31356607822164	5.04334610165708
C	-0.17695203809585	0.01507758502380	6.51527224383696
H	0.64011398389728	-0.63195169559688	6.84061751856879
H	-1.02984307437984	-0.15119760042166	7.17748422396941
H	0.14227310715242	1.05180188786757	6.63932150853459
C	-1.73268538651514	0.61802999174966	4.61476315236979
H	-1.43459644967519	1.66897344958843	4.62815761083863
H	-2.58678435698326	0.50145928314825	5.28637408194421
H	-2.05816254589636	0.37639660973939	3.60046865410838
C	2.62441745990733	-2.28679953307380	1.61049651300737
H	2.31419192121884	-3.20033635029035	2.12604130584230
C	4.13619232307871	-2.37531281593207	1.37992312380219

H	4.50174796938005	-1.55137441386553	0.76302504228109
H	4.37729996357541	-3.30453911049231	0.85947274337744
H	4.68361599542521	-2.36014956314187	2.32444760309750
C	1.87331224167759	-2.24503664573726	0.26820301917178
H	0.79186171995442	-2.23573935175311	0.41610750552012
H	2.12583158898912	-3.11682216673009	-0.34043058522611
H	2.14490248953008	-1.34691525691072	-0.29263275905882
C	-5.07235395963511	-5.06305127752083	2.06826877504698
H	-5.60632739407842	-4.10971548388874	2.09783209891430
C	-7.04659922736434	-6.10272969018020	1.44615626702420
C	-7.92895862385975	-6.88471579549750	2.22656809643002
C	-9.28775324180640	-6.82893671718632	1.92826423060065
H	-9.97963610915967	-7.40293487799170	2.53364352513342
C	-9.77089886551700	-6.06145534747181	0.87413870203989
H	-10.83275901363214	-6.03371053219067	0.66269282733860
C	-8.88403098033039	-5.34955032069676	0.08392135390269
H	-9.26168980873996	-4.77622009086477	-0.75350293960778
C	-7.51045421264360	-5.35490958016726	0.34118039453801
C	-7.47657487049633	-7.77658192029095	3.37615907264438
H	-8.39485987660406	-8.21669673547838	3.77505360827966
C	-6.81708306168798	-7.01903266574107	4.53980470774067
H	-7.41146719390805	-6.15159159804492	4.83575552763302

H	-6.72783918331339	-7.67970477510040	5.40546939400690
H	-5.81614088495691	-6.67528799094299	4.28025042806810
C	-6.59596121893788	-8.94539750869583	2.90509300176436
H	-6.38897428970494	-9.61629904167160	3.74249096963988
H	-5.64527231828552	-8.58804188663960	2.51047030440196
H	-7.09690248280513	-9.52161550641452	2.12437422753078
C	-6.58232723876727	-4.61072292054029	-0.61264743896551
H	-5.55121438446962	-4.84241303432238	-0.34708274252752
C	-6.77082775297031	-5.08023570129668	-2.06442738417349
H	-6.64017194804576	-6.16109207768391	-2.14538146887034
H	-6.03586053291528	-4.59700640092145	-2.71233821972986
H	-7.76355962754980	-4.82947929124792	-2.44289334086400
C	-6.75374551435202	-3.08750172476076	-0.50706209104996
H	-7.77086612158090	-2.78882451851861	-0.77062021406200
H	-6.06654740891491	-2.57864008295329	-1.18763672453153
H	-6.55819807186977	-2.73196910828746	0.50773479071466
C	-0.87856473489482	-7.53129249429065	3.47025822435203
C	-0.41253795067750	-7.42779418251529	4.93790682353139
H	0.12117660798739	-8.33760314031947	5.22028207317819
H	-1.26721737367734	-7.30999850528899	5.60761244657976
H	0.26002508174186	-6.58200738037550	5.08912365088799
C	0.34795625565335	-7.69694771689058	2.54916592538481

H	0.04189302518407	-7.75906290417482	1.50256416467228
H	0.87854578881189	-8.61637672174970	2.80486771638850
H	1.04995560622924	-6.86819625226978	2.65126654574972
C	-1.76800315130418	-8.77464822411070	3.32620125619605
H	-2.12035674402208	-8.90347911870144	2.30048735800598
H	-2.63625049632030	-8.73188723949678	3.98699904796507
H	-1.19117764056814	-9.66113019771801	3.59404079308062
N	0.36927504845247	-2.47143564690022	3.26627457433458
N	-5.67516908522178	-6.13974266510745	1.77801871320000
O	-3.54134315326342	-2.60425199839178	2.12759170367104
H	-3.90331088226120	-2.52663260556039	1.22054602327758
H	-4.17934942674100	-2.26411301561024	2.78865268046933

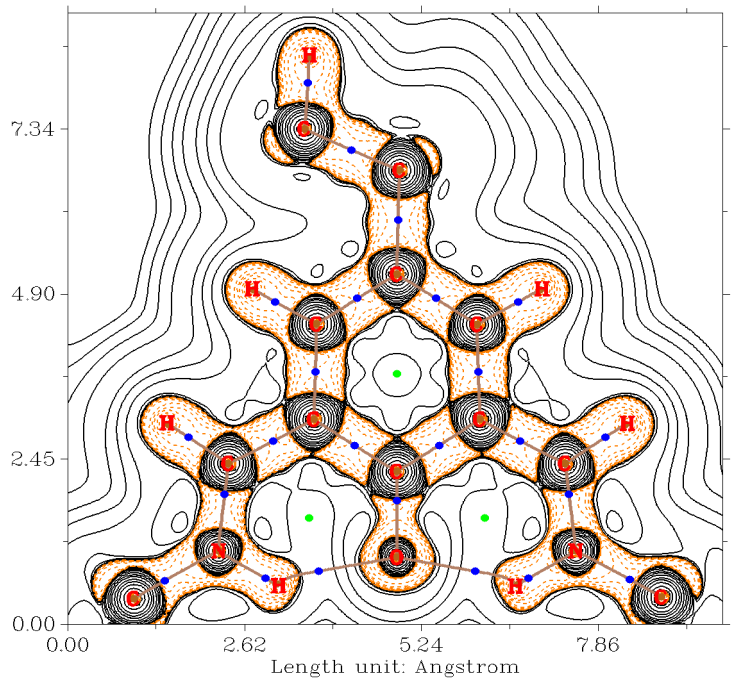

Figure S30. Contour map of the Laplacian ($\nabla^2\rho(\mathbf{r})$) of electron density of $[H_2{}^{t\text{Bu,Dipp}}L]^+$ - plotted in the plane of the central benzene ring. The solid (black) and dashed (orange) lines correspond to positive and negative Laplacian values respectively. The blue (●) and green (●) dots mark bonding (3,–1) and ring (3,+1) critical points respectively.

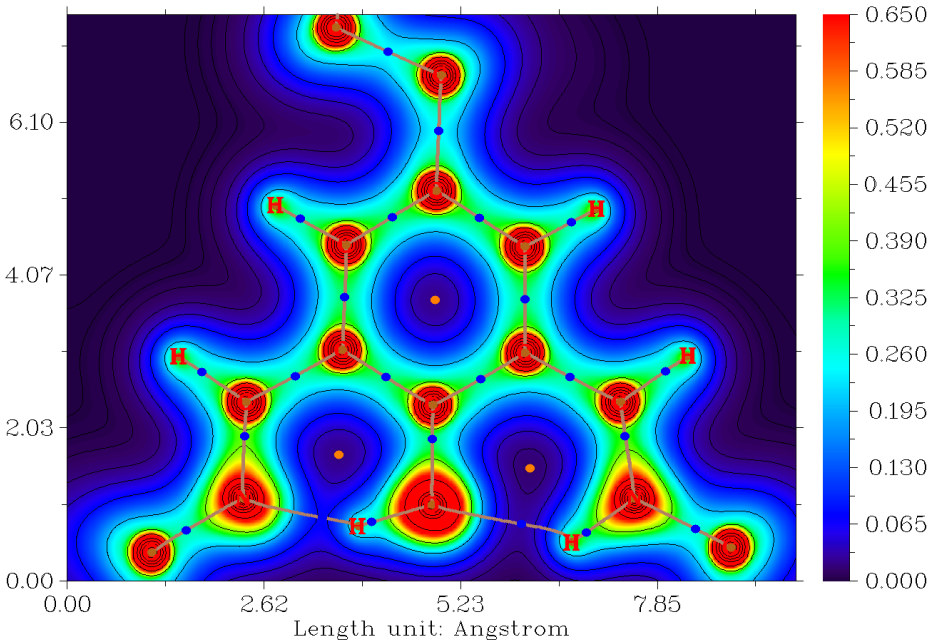

Figure S31. Contour map of the electron density of $[H_2{}^{t\text{Bu,Dipp}}L]^+$ in the alternative [N<OH>NH]$^+$ form - plotted in the plane of the central benzene ring. The blue (●) and orange (●) dots mark bonding (3,–1) and ring (3,+1) critical points respectively.

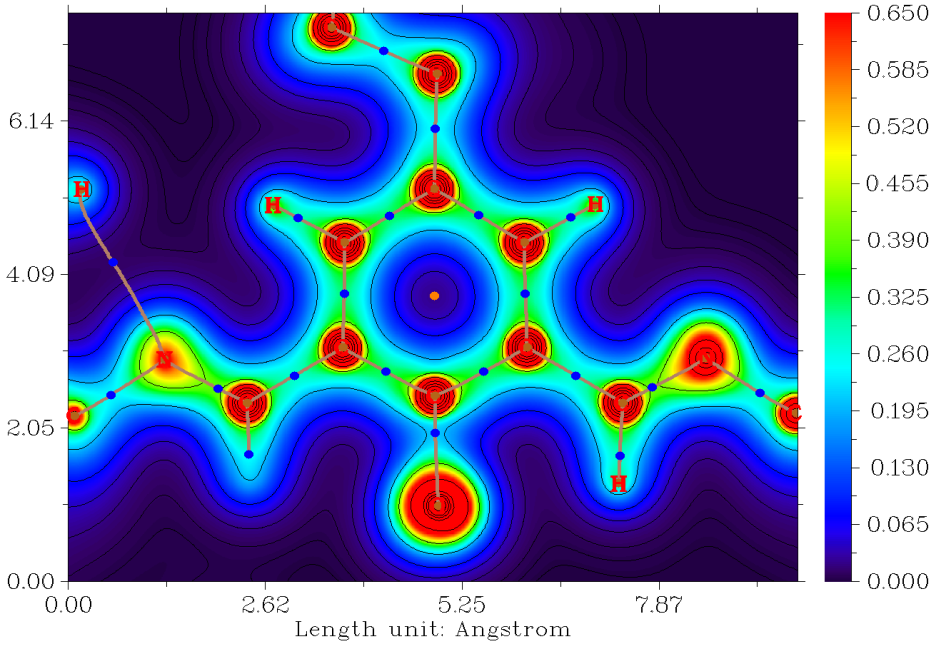

Figure S32. Contour map of the electron density of $[H_2{}^{t\text{Bu,Dipp}}L]^+$ in the least favoured $[N<OH_2>N]^+$ form - plotted in the plane of the central benzene ring. The blue (•) and orange (•) dots mark bonding (3,–1) and ring (3,+1) critical points respectively.

Calculating hydrogen bond energies:

The energy associated with the hydrogen bonding interactions within these systems was estimated using the methods reported by Lu *et al.*[29] These take into account the electron density at the bonding critical point of the hydrogen bonds:

- For a neutral hydrogen bond: $\Delta E \approx -223.08 \times \rho(\boldsymbol{r}_{BCP}) + 0.7423$
- For a charged hydrogen bond: $\Delta E \approx -332.34 \times \rho(\boldsymbol{r}_{BCP}) - 1.0661$

These equations were determined to be more accurate than the original energy predictor proposed by Espinosa in 1998 which instead utilised the potential energy at the bonding critical points[30]: $\Delta E \approx \frac{V(\boldsymbol{r}_{BCP})}{2}$.

VI. References

1. L. F. Lindoy, G. V. Meehan and N. Svenstrup, *Synthesis*, 1998, 1029-1032.
2. P. D. Knight, A. J. P. White and C. K. Williams, *Inorg. Chem.*, 2008, **47**, 11711-11719.
3. L. Wang, W.-H. Sun, L. Han, Z. Li, Y. Hu, C. He and C. Yan, *J. Organomet. Chem.*, 2002, **650**, 59-64.
4. S. J. Lancaster, A. Rodriguez, A. Lara-Sanchez, M. D. Hannant, D. A. Walker, D. H. Hughes and M. Bochmann, *Organometallics*, 2002, **21**, 451-453.
5. T. Rodima, V. Mäemets and I. Koppel, *J. Chem. Soc., Perkin Trans. 1*, 2000, 2637-2644.
6. S. Tshepelevitsh, A. Kütt, M. Lõkov, I. Kaljurand, J. Saame, A. Heering, P. G. Plieger, R. Vianello and I. Leito, *Eur. J. Org. Chem.*, 2019, 6735-6748.
7. A. Kütt, S. Tshepelevitsh, J. Saame, M. Lõkov, I. Kaljurand, S. Selberg and I. Leito, *Eur. J. Org. Chem.*, 2021, **2021**, 1407-1419.
8. J. Cosier and A. M. Glazer, *J. Appl. Crystallogr.*, 1986, **19**, 105-107.
9. *Journal*, CrysAlisPRO, Oxford Diffraction /Agilent Technologies UK Ltd, Yarnton, England.
10. A. Altomare, G. Cascarano, C. Giacovazzo and A. Guagliardi, *J. Appl. Crystallogr.*, 1993, **26**, 343-350.
11. L. Palatinus and G. Chapuis, *J. Appl. Crystallogr.*, 2007, **40**, 786-790.
12. L. Farrugia, *J. Appl. Crystallogr.*, 1999, **32**, 837-838.
13. P. W. Betteridge, J. R. Carruthers, R. I. Cooper, K. Prout and D. J. Watkin, *J. Appl. Crystallogr.*, 2003, **36**, 1487.
14. A. Spek, *J. Appl. Crystallogr.*, 2003, **36**, 7-13.
15. L. Farrugia, *J. Appl. Crystallogr.*, 1997, **30**, 565.
16. F. Neese, F. Wennmohs, U. Becker and C. Riplinger, *The Journal of Chemical Physics*, 2020, **152**, 224108.
17. F. Neese, *WIREs Computational Molecular Science*, 2012, **2**, 73-78.
18. F. Neese, *WIREs Computational Molecular Science*, 2022, **12**, e1606.
19. A. D. Becke, *The Journal of Chemical Physics*, 1986, **84**, 4524-4529.
20. C. Lee, W. Yang and R. G. Parr, *Physical Review B*, 1988, **37**, 785-789.
21. A. D. Becke, *The Journal of Chemical Physics*, 1993, **98**, 5648-5652.
22. D. A. Pantazis, X.-Y. Chen, C. R. Landis and F. Neese, *Journal of Chemical Theory and Computation*, 2008, **4**, 908-919.

23. D. A. Pantazis and F. Neese, *Journal of Chemical Theory and Computation*, 2009, **5**, 2229-2238.
24. S. Grimme, J. Antony, S. Ehrlich and H. Krieg, *The Journal of Chemical Physics*, 2010, **132**, 154104.
25. F. Neese, F. Wennmohs, A. Hansen and U. Becker, *Chem. Phys.*, 2009, **356**, 98-109.
26. R. Izsák and F. Neese, *The Journal of Chemical Physics*, 2011, **135**, 144105.
27. E. F. Pettersen, T. D. Goddard, C. C. Huang, G. S. Couch, D. M. Greenblatt, E. C. Meng and T. E. Ferrin, *J. Comput. Chem.*, 2004, **25**, 1605-1612.
28. T. Lu and F. Chen, *J. Comput. Chem.*, 2012, **33**, 580-592.
29. S. Emamian, T. Lu, H. Kruse and H. Emamian, *J. Comput. Chem.*, 2019, **40**, 2868-2881.
30. E. Espinosa, E. Molins and C. Lecomte, *Chem. Phys. Lett.*, 1998, **285**, 170-173.